

**PERFORMANCE EVALUATION OF HELICAL TURBINE**

A dissertation submitted in partial fulfilment of the requirement for the award of degree of

**MASTER OF TECHNOLOGY**

**IN**

**HYDRAULICS AND WATER RESOURCES ENGINEERING**

**BY**

**AJAY KUMAR**

(ROLL NO. 2K15/HFE/03)

**Under the guidance of**

**Dr. BHARAT JHAMNANI**

**Asst. Professor**

**Department of Civil Engineering**

**Delhi Technological University**

**Delhi**



**DELHI TECHNOLOGICAL UNIVERSITY  
(FORMERLY DELHI COLLEGE OF ENGINEERING)**

**DELHI-110042**

**JULY-2017**



## **CANDIDATES'S DECLARATION**

I do hereby certify that the work presented is the report entitled “**performance evaluation of helical turbine**” in the partial fulfilment of the requirements for the award of the degree of “master of technology” in hydraulics & water resources engineering submitted in the department of civil engineering, Delhi Technological University, is an authentic record of our own work carried out from January 2017 to June 2017 under supervision of Dr. Bharat Jhamnani (Asst.professor),department of civil engineering.

I have not submitted the matter embodied in the report for the award of other degree or diploma.

Date:

Ajay Kumar  
(2k15/HFE/03)

### **Certificate**

This is to certify that above statement made by the candidate is correct to best of my knowledge.

Dr. Bharat Jhamnani  
(Asst. Professor)  
Department of Civil Engineering  
Delhi Technological University

## **ACKNOWLEDGEMENT**

I take this opportunity to express my profound gratitude and deep regards to Dr. Bharat Jhamnani(Asst. Professor, Civil Engineering Department, DTU) for his exemplary guidance, monitoring and constant encouragement throughout the course for this project work. The Guidance and help given by him from time to time shall carry me a long way in life on which I am going to embark.

I would also like to thank Dr. Nirendra Dev (Head of Department, Civil Engineering Department, DTU), Professors and faculties of the department of Civil Engineering, DTU, who have always extended their full co-operation and help. They have been kind enough to give their opinions on the project matter; I am deeply obliged to them. They have been a source of encouragement and have continuously been supporting me with their knowledge base, during study. Several of well wishers extended their help to me directly or indirectly and we grateful to all of them without whom it would have been impossible for me to carry on my work.

## TABLE OF CONTENTS

CANDIDATES’S DECLARATION .....	II
ABSTRACT.....	VI
Chapter 1 INTRODUCTION.....	- 1 -
1.1. Power generation in India .....	- 1 -
1.2.2 Classification based on the operation .....	- 2 -
1.2.3 Classification based on storage: .....	- 2 -
1.2.4 Classification on the basis of power capacity.....	- 3 -
1.3 Turbines used in Hydro electric stations:.....	- 3 -
1.4 Helical Turbine.....	- 4 -
1.5 Objectives of study:.....	- 5 -
Chapter 2 LITERATURE REVIEW .....	- 7 -
2.1.Gorlov Helical turbine.....	- 7 -
2.2 Fluid Performance .....	- 8 -
2.3 Turbine axis-orientation .....	- 9 -
2.4 Environmental issues.....	- 9 -
2.5 Working principle of helical turbine .....	- 9 -
2.2.2. Tip speed ratio: It is the ratio of tangential speed of the tip of the blade and the actual speed of the wind. It is denoted by $\lambda$ <sup>[13]</sup> .....	- 11 -
2.2.3. Moment coefficient: It is a dimensionless number that comes in wind turbine aerodynamics which is denoted by $C_m$ <sup>[13]</sup> .....	- 11 -
2.7 Status of research work done on helical turbine .....	- 11 -
Chapter 3 METHODOLOGY.....	- 15 -
3.1 Introduction .....	- 15 -
3.1.1 Ansys fluent:.....	- 15 -
3.1.2 Hydrofoil coordinates:.....	- 16 -
3.2 Discretization. ....	- 24 -
3.3 Governing equation:.....	- 26 -
3.4. Calculation of $C_L$ , $C_D$ and $C_m$ : .....	- 29 -
3.5 Boundary conditions: .....	- 30 -
Chapter 4 RESULTS AND DISCUSSION .....	- 32 -
4.1. Model Validation.....	- 32 -
4.2 Variation of $C_m$ with change in enclosures .....	- 32 -

4.3 Performance evaluation of helical turbine under varying conditions: .....	- 36 -
4.3.1. By varying inlet and angular velocity: .....	- 36 -
4.3.2. Performance evaluation by change in volume of turbine: .....	- 37 -
4.5. Exploration of a possibility of spacing several helical turbines in a line in a river for the purpose of hydropower generations: .....	- 40 -
4.6. Effects of helical turbine operation in variation of flow velocity in channel upstream and downstream side. ....	- 48 -
Chapter 5 CONCLUSIONS .....	- 52 -
REFERENCES .....	- 53 -

## **ABSTRACT**

Helical turbines are generally in wind turbine but now it has been widely used in tidal hydroelectric power plants since it starts rotating at a very low velocity ranging from 1.2 m/s to 5.5 m/s. Power from the same turbine can also be extracted out of flowing water from small river tributaries and canals. A numerical study has been done with the help of CFD on a design of a helical turbine given in the journal published by Gorlov. The same Gorlov helical turbine was modelled as well as its efficiency results are validated using CFD tool i.e. Ansys fluent 15.0. Performance analysis was also done by varying boundary conditions such as inlet velocity from 1.5 m/s to 2.5 m/s with a step size of 0.25 m/s and angular velocity from 100 rpm to 150 rpm with a step size of 10 rpm. Thereafter ten different models were designed by just varying the dimensions of the Gorlov helical turbine such as its diameter and height and their Performance analysis was done. Performance analysis was then done on the these ten models when they are installed at a spacing of 5 to 15 metres with a step size of 2.5 metres and the required spacing were found for the ten turbines and a linear regression model was developed between the turbine (taking its volume) and the desired spacing. Besides this, the variation in the flow velocity in upstream and downstream of a helical turbine in channel was also found when turbine operates.

## LIST OF FIGURES

Figure 1.1 Helix shape .....	- 4 -
Figure 1.2 Helical turbine model .....	- 5 -
Figure 1.3 Helical turbine instalallation on flowing river in South Korea .....	- 5 -
Figure 2.1 Darieus turbine .....	- 7 -
Figure 2.2 Helical wind turbine .....	- 7 -
Figure 2.3 a) Straight blades,b) helical blades .....	- 8 -
Figure 2.4 Position of hydrofoil cross section in helical turbine .....	- 8 -
Figure 2.5 a) Current flow to left, b) Induced flow component.....	- 10 -
Figure 2.6 a) Apparent flow velocity at blade, b) Net force vector .....	- 10 -
Figure 3.1 Foil details .....	- 16 -
Figure 3.2 Drawing detailing of hydrofoil .....	- 22 -
Figure 3.3 Hydrofoil coordinates sketch.....	- 22 -
Figure 3.4 Base plate sketch .....	- 22 -
Figure 3.5 Base plate sketch with hydrofoil .....	- 23 -
Figure 3.6 Plan of swept model of helical blades .....	- 23 -
Figure 3.7 Elevation of swept model of helical blades .....	- 23 -
Figure 3.8 Enclosure detailing .....	- 24 -
Figure 3.9 Turbine model with enclosures .....	- 24 -
Figure 3.10 Mesh figure.....	- 25 -
Figure 3.11 Inlet section .....	- 25 -
Figure 3.12 Outlet section.....	- 25 -
Figure 3.13 Wall section .....	- 26 -
Figure 3.14 Control volume discretization. ....	- 29 -
Figure 4.1 Variation of $C_m$ with change in enclosure 1 .....	- 34 -
Figure 4.2 $C_m$ variation under steady condition.....	- 34 -
Figure 4.3 $C_m$ variation under transient condition .....	- 35 -
Figure 4.4 Velocity vectors.....	- 35 -
Figure 4.5 Velocity streamlines .....	- 36 -
Figure 4.6 $C_m$ variation on varying inlet velocity and angular velocity .....	- 37 -
Figure 4.7 $V_1$ Model .....	- 38 -
Figure 4.8 $C_m$ variation with change in volume of turbine.....	- 39 -
Figure 4.9 Helical position in design modeller .....	- 40 -
Figure 4.10 Enclosure in design modeller .....	- 41 -
Figure 4.11 Velocity vectors contour for 5 m spacing.....	- 41 -
Figure 4.12 Velocity vectors contour for 7.5 m spacing.....	- 41 -
Figure 4.13 Velocity vectors contour for 10 m spacing.....	- 42 -
Figure 4.14 Velocity vectors contour for 12.5 m spacing.....	- 42 -
Figure 4.15 Velocity vectors contour for 15 m spacing.....	- 42 -
Figure 4.16 Graph on desired spacing with the variation in volume of turbine .....	- 48 -
Figure 4.17 Mesh diagram for 40 m channel .....	- 49 -
Figure 4.18 Inlet for 40 m channel model.....	- 49 -

Figure 4.19 Outlet for 40 m channel model ..... - 49 -  
Figure 4.20 Velocity streamlines for 40 m channel ..... - 50 -  
Figure 4.21 Velocity variation chart for channel in downstream of turbine..... - 50 -  
Figure 4.22 Velocity chart for channel in upstream of turbine..... - 50 -



## LIST OF TABLES

Table 1.1 Sources of power generation capacity in India .....	- 1 -
Table 1.2 Tidal power production across the world .....	- 2 -
Table 1.3 Classification on the basis of power capacity .....	- 3 -
Table 1.4 Turbine selection on the basis of head .....	- 3 -
Table 1.5 power production detailing from a Kaplan turbine.....	- 4 -
Table 3.1 Gorlov Helical turbine dimensions .....	- 15 -
Table 3.2 NACA-0020 coordinate table for 7 inch chord .....	- 17 -
Table 3.3 Boundary Conditions .....	- 30 -
Table 4.1 Validation table.....	- 32 -
Table 4.2 variation of $C_m$ with change in enclosures.....	- 33 -
Table 4.3 Variation of $C_m$ on varying inlet & angular velocity .....	- 36 -
Table 4.4 Ten different helical turbine models detailing .....	- 38 -
Table 4.5 Variation of $C_m$ by varying turbine dimensions .....	- 39 -
Table 4.6 Variation of $C_{m-1}$ & $C_{m-2}$ with change in spacing for model $V_1$ .....	- 43 -
Table 4.7 Variation of $C_{m-1}$ & $C_{m-2}$ with change in spacing for model $V_2$ .....	- 43 -
Table 4.8 Variation of $C_{m-1}$ & $C_{m-2}$ with change in spacing for model $V_3$ .....	- 44 -
Table 4.9 Variation of $C_{m-1}$ & $C_{m-2}$ with change in spacing for model $V_4$ .....	- 44 -
Table 4.10 Variation of $C_{m-1}$ & $C_{m-2}$ with change in spacing for model $V_5$ .....	- 45 -
Table 4.11 Variation of $C_{m-1}$ & $C_{m-2}$ with change in spacing for model $V_6$ .....	- 45 -
Table 4.12 Variation of $C_{m-1}$ & $C_{m-2}$ with change in spacing for model $V_7$ .....	- 46 -
Table 4.13 Variation of $C_{m-1}$ & $C_{m-2}$ with change in spacing for model $V_8$ .....	- 46 -
Table 4.14 Variation of $C_{m-1}$ & $C_{m-2}$ with change in spacing for model $V_9$ .....	- 47 -
Table 4.15 Variation of $C_{m-1}$ & $C_{m-2}$ with change in spacing for model $V_{10}$ .....	- 47 -

## LIST OF SYMBOLS

<b>Symbol</b>	<b>Title</b>
$\omega$	angular velocity
$\rho$	density of water
$\lambda$	tip speed ratio
$C_p$	power coefficient
$C_m$	moment coefficient

# Chapter 1 INTRODUCTION

## 1.1. Power generation in India

Energy crisis is one of the problems we are facing in our country. Although we are exploring new options like nuclear energy, solar energy, wind energy etc, But we could not explore the tapped capacity of 1,75,000MW hydro energy from our rich water resources, till today we have just explored around 30000 MW only<sup>(1)</sup>.

India's total power generation capacity as on 30<sup>th</sup> June 2016 was 3, 03,118.21 MW, which includes following:

**Table 1.1** Sources of power generation capacity in India

Source of power production	Power production(MW)	%
Coal	1,92,168.88	60.13
Gas	25,329.38	7.95
Diesel	837.63	0.26
Nuclear	6780.00	2.12
Hydel	44,478.42	13.92
Wind and sun energy	50,018.00	15.65

Of all these Hydro energy is the cheapest and clean energy but the problem that we face in its exploration are initial DPR which takes time due to initial technical complexities and heavy initial investment plus opposition of the projects by local inhabitants which often causes crisis due to land submergence and rehabilitations issues and at last its construction time that its takes.

## 1.2 Classification of hydro energy tapping procedures

### 1.2.1 Its main Classification is based on hydraulic structures

i) **Conventional hydroelectric plant:** Dams are constructed across the rivers to have a potential head which could be used to convert kinetic energy. This further classified on the

basis of their heads as low head(less than 15 m), medium head (15-70m), high head(70-250m) and very high head more than(250m).

ii) **Pumped storage plants:** In this type of plants the same water is used again and again by pumping back it during the off peak hours. They are mainly used to meet the peak demand.

iii) **Tidal plants:** Tidal power plants are constructed on oceans where tidal rise and fall are used to create potential heads. A dam is constructed on a suitable location to obstruct the rise and fall of tides and thereafter the head developed on the either side of the dam are used for the generation of power. In a day two rise and two fall are occur from where heads can be developed but since rise and fall occurs are of 1 to 2 m therefore high velocity is difficult to achieve due to which we use helical turbine. Till now helical turbines has been used for tidal power plants across the world as follows:

**Table 1.2** Tidal power production across the world

Country	Installed power(MW)
Russia	0.4
Canada	18
China	3.9

### 1.2.2 Classification based on the operation

i) **Base load plants:** This type of plants involves in continuous power generation. Simply speaking conventional hydroelectric power plants are base load plants.

ii) **Peak load plants:** If the power plant is operated only to meet the peak demand then it is called peak load plants. In general, pumped storage power plants are peak load plants. In this type of hydroelectric power plants the same water is utilized again and again by pumping back during the off peak hours.

### 1.2.3 Classification based on storage:

i) **With Storage reservoir:** If the availability of the water is uneven over the year, storage reservoirs are essential

ii) **Without storage reservoir:** Also known as run off river plants. If there is a natural normal flow throughout the year then it is not essential to have a reservoir. Under such conditions a mini reservoir or pond that takes care of day to day fluctuations is enough.

### 1.2.4 Classification on the basis of power capacity

**Table 1.3** Classification on the basis of power capacity

Type	Capacity
Micro hydro electric plants	< 100 kW
Mini hydro electric plants	100kW to 1MW
Small hydro electric plants	1 MW to a few MW
Medium hydro electric plants	More than a few MW
Super hydro electric plants	More than 1000 MW

### 1.3 Turbines used in Hydro electric stations:

Various types of turbines used in hydro power stations are shown in table below.

**Table 1.4** Turbine selection on the basis of head

Head in metres	Type of turbine
300 or more	Pelton wheel or Multiple jet
150 or 300	Pelton or Francis
60 to 150	Francis or Deriaz
Less than 60	Kaplan or propeller or Deriaz or Tubular

Here Pelton wheel and Multiple jet type are impulse turbines in which all the available energy of water is converted into kinetic energy or velocity head. Whereas other turbines are reaction type where only a part of the available energy of water is converted into kinetic energy and a major part remains in the form of pressure energy. As far as the relation of type of turbine used for a certain discharge is directly depends on the head available from the equation as:

$$P = \gamma Q H \quad \dots 1.1$$

Where  $\gamma$  is the specific weight of water

Q is the discharge in  $m^3/s$

H is the net head available

Since discharge requirement for pelton wheel is less as compared to discharge requirement for Francis turbine if we have to extract the same amount of power from both the turbines, discharge for Francis gets increased as head available in this case is less, as it can be easily analysed from equation 1.1. That means to extract more power both the discharge and head

has to be more as per equation 1.1. Power production from one of the Kaplan turbines has been shown below where it can be easily analysed the increase in power production with increase in both head and discharge.

**Table 1.5** power production detailing from a Kaplan turbine

Head(metre)	Discharge (cumec)	Approx. Power production(watts)	Pipe Size(metres)
0.3048	0.020192	25	0.0203(minimum)
0.6096	0.028395	70	0.02032
0.9144	0.034705	150	0.0254
1.2192	0.0400685	250	0.0254
1.524	0.044801	350	0.0254
1.8288	0.0489025	465	0.03048
2.1336	0.053004	585	0.03048
2.4384	0.0564745	715	0.03048
2.7432	0.059945	850	0.03048
3.048	0.0631	1000	0.03048

Besides this turbines used in low velocity from 1.2 m/s to 5.5 m/s as we get in tidal power plants are helical turbine and As being said by Gorlov <sup>[7]</sup> that torque production from the helical turbine increases when the volume of water passing through helical turbine even when the torque radius is kept constant i.e its diameter is kept unchanged and its height is being increased. It is because the swept area of the turbine blades increases with increase in height as well as diameter.

### 1.4 Helical Turbine

The word helical refers to something which is in the shape of a helix, which means to say that it is in the form of a wound spiral. As shown in the figure 1.1 below that depicts the mathematical description of a helix.



**Figure 1.1** Helix shape

Helical turbines come in different makes and designs but the basic principle of operation is the same. One such design has been shown below.

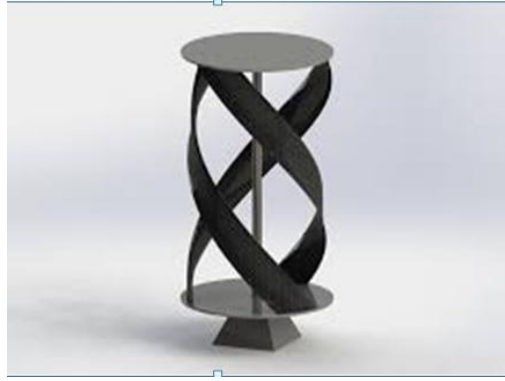


**Figure 1.2** Helical turbine model

The helical turbine model came after modification done over straight blades Darieus wind turbine. This was later designed for hydro energy and got patented by Professor Gorlov of Boston. Since in dams there is a potential head that gets converted to high velocity to run a turbine. But what if we explore the kinetic energy of the running flow of a river tributaries or canals where the velocity is not high as required for Kaplan or propeller turbines. Therefore a consideration has been given to helical turbine which can run even at low velocity and which can be installed in the flowing direction which otherwise is going as waste. Since Gorlov helical turbine is used for low-head micro hydro installations, when construction of a dam is undesirable therefore we have considered Gorlov helical turbine. Gorlov helical turbine is a hydrokinetic turbine which runs on flowing water even when the speed of water is 1.2 m/s. till today helical turbines has been installed in wind energy and tidal energy, and its installation on flowing river or canal has been done in either in US and south Korea and that too on small scale itself. One of such installation has been shown in figure 1.3.



**Figure 1.3** Helical turbine instalallation on flowing river in South Korea

### **1.5 Objectives of study:**

- 1) Formulation of numeric model of Gorlov turbine using CFD analysis tools ansys 15.0.
- 2) Validation of numeric CFD model using published literature.

- 3) Determination of energy efficiency using CFD analysis.
- 4) Evaluation of hydraulic performance of helical turbine under varying conditions of operations through cfd analysis.
- 5) Exploration of a possibility of placing several such turbines in a line in a river at appropriate spacing for the purpose of hydropower generations
- 7) Effects of helical turbine operation in variation of flow velocity in channel upstream and downstream.



## Chapter 2 LITERATURE REVIEW

### 2.1.Gorlov Helical turbine.

Helical turbines have come after design modifications on Darrieus turbines. Darrieus turbines are wind turbines with straight blades of some foil shape.



**Figure 2.1** Darrieus turbine

whereas when the straight blades are modified to a helical shape, it becomes a helical turbine.



**Figure 2.2** Helical wind turbine

## 2.2 Fluid Performance

Foil term used here is a cross section of the blade of the turbine which is termed as aerofoil or hydrofoil depending upon the fluid interaction as air or water respectively. fluid interaction with the foil gives drag to blade which itself depends on velocity of fluid and it rotates the blades.

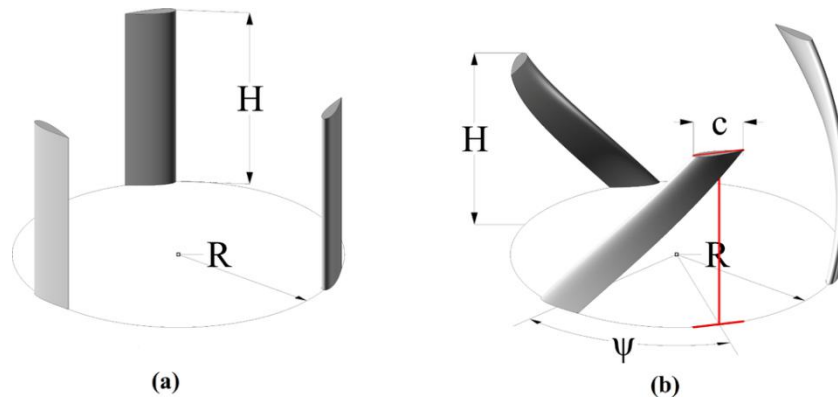


**Figure 2.3** a) Straight blades, b) helical blades

Due to straight blades in darieus turbine self starting problem occurs as wind flow never remains in the same direction and for the rotation of the blades foils has to be normal to the flow of fluid. Due to this problem blades were modified to helical shape so that at any point of time one shape will always be inclined normal to the direction the flow and whatever be the direction of flow. also fluctuation of torque is there in dariues turbine whereas due unifromly distributed foils constant torque is generated in helcial turbines.

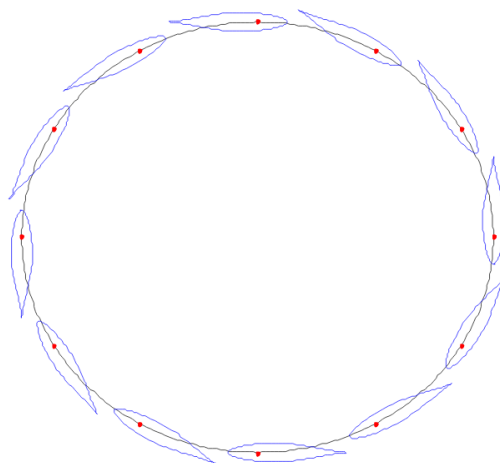


**Figure 2.4** Position of hydrofoil cross section in helical turbine

both the helical and darieus turbine uses velocity head of the flowing fluid i.e.  $V^2/2g$ .

### **2.3 Turbine axis-orientation**

When we compare a helical turbine with a conventional turbine the main difference lies with its axis of axis of rotations. helical turbines can be vertical as well as horizontal axis turbine whereas conventional turbine are horizontal axis turbines i.e the turbines axis are places horizontal to the flow of current. Gorlov helical is a vertical-axis turbine which means the axis is positioned perpendicular to current flow, whereas traditional turbines are horizontal-axis turbines which means the axis is positioned parallel to the flow of the current. Fluid flows, such as wind, will naturally change direction, however they will still remain parallel to the ground. So in all vertical-axis turbines, the flow remains perpendicular to the axis, regardless of the flow direction, and the turbines always rotate in the same direction. This is one of the main advantages of vertical-axis turbines.

### **2.4 Environmental issues**

Gorlov helical turbine is proposed for low-head micro hydro installations, when construction of a dam is undesirable. The Gorlov helical turbine is an example of damless hydro technology. The technology may potentially offer cost and environmental benefits over dam-based micro-hydro systems.

Some advantages of damless hydro are that it eliminates the potential for failure of a dam, which improves public safety. It also eliminates the initial cost of dam engineering, construction and maintenance, reduces the environmental and ecological complications, and potentially simplifies the regulatory issues put into law specifically to mitigate the problems with dams.

As far as environmental issues are concerned the helical turbine donot require dam wheras conventional turbines require dams which has various environmental impacts. caviations problems occurs in conventional turbines whereas no such problems are there in helcal turbines.

### **2.5 Working principle of helical turbine**

Here the direction of the fluid flow is to the left as shown in figure 2.5(a). As the turbine rotates, in this case in a clockwise direction, the motion of the foil through the fluid changes the apparent velocity and angle of attack (speed and direction) of the fluid with respect to the frame of reference of the foil. The combined effect of these two flow components (i.e. the vector sum), yields the net total "Apparent flow velocity" as shown in the figure 2.7.

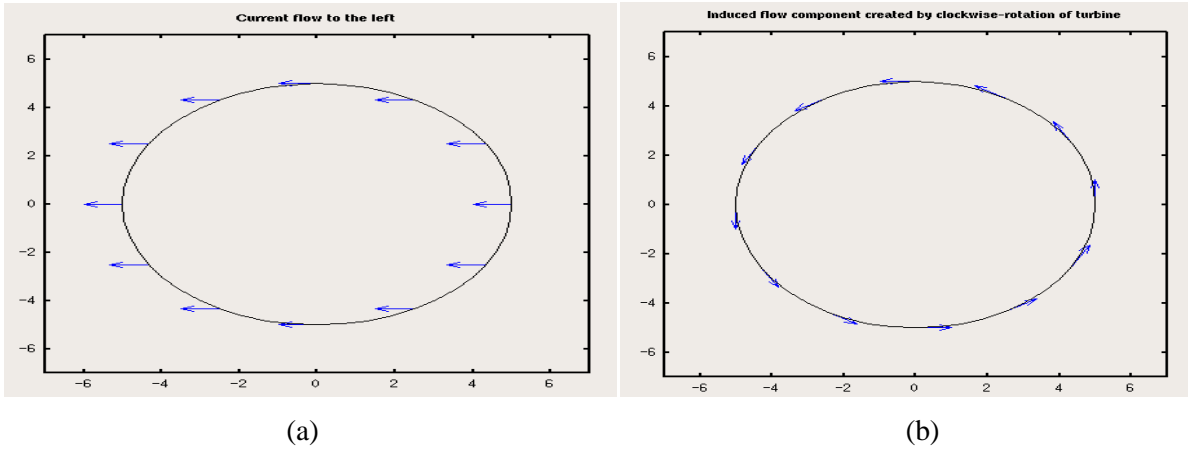


**Figure 2.5** a) Current flow to left, b) Induced flow component

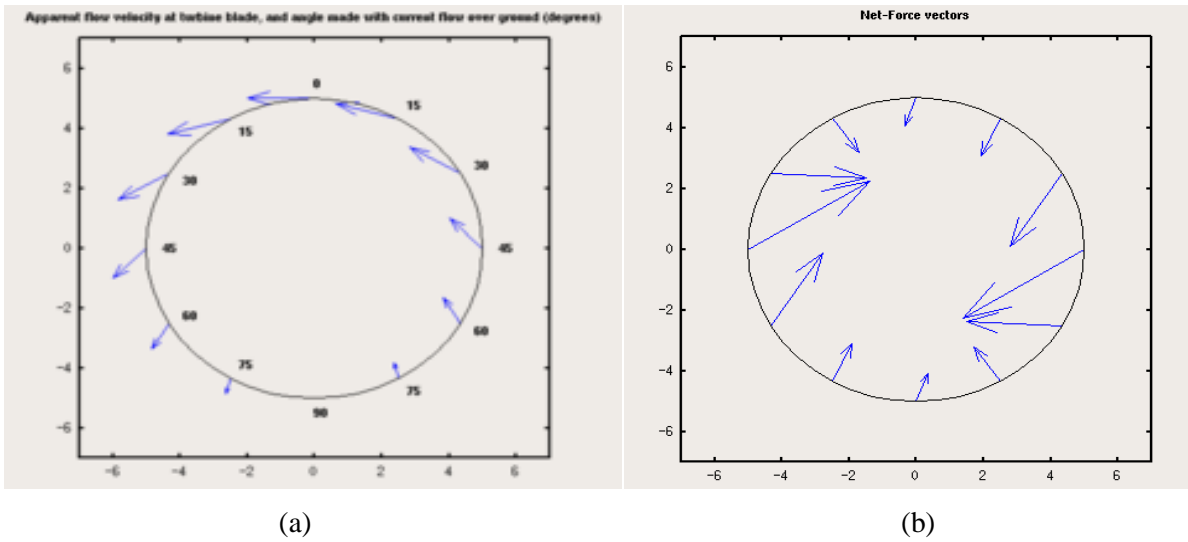


**Figure 2.6** a) Apparent flow velocity at blade, b) Net force vector

The action of this apparent flow on each foil section generates both a lift and drag force, the sum of which is shown in the figure 2.6(b). Each of these net force vectors can be split into two orthogonal vectors as a radial component and a tangential component, shown here as "Normal force" and "Axial force" respectively. The normal forces are opposed by the rigidity of the turbine structure and do not impart any rotational force or energy to the turbine. The remaining force component propels the turbine in the clockwise direction, and it is from this torque that energy can be harvested.

## 2.6. Power Efficiency calculation of helical turbine:

**2.2.1. Power coefficient:** Helical turbine was initially used as wind turbines therefore power coefficient term has been used in spite of efficiency, both are synonymous. Power coefficient is the product of tip-speed ratio and moment coefficient <sup>[13]</sup>.

$C_p = \text{output power/input power}$

$$C_p = T\omega/0.5\rho AV^3 \quad \dots 2.1$$

Where T is torque in  $N \cdot m$ ,  $\rho$  is air density in  $kg/m^3$ , A is turbine area in  $m^2$ , and V is velocity of flow in  $m/s$

**2.2.2. Tip speed ratio:** It is the ratio of tangential speed of the tip of the blade and the actual speed of the wind. It is denoted by  $\lambda$  [13].

$$\lambda = \text{tip speed/wind speed} = \omega R/V = \omega D/2V \quad \dots 2.2$$

Where  $\omega$  is angular velocity in Rad/s, V is velocity of fluid in m/s

**2.2.3. Moment coefficient:** It is a dimensionless number that comes in wind turbine aerodynamics which is denoted by  $C_m$  [13].

$$C_m = T/0.25\rho ADV^4 \quad \dots 2.3$$

Where A is the swept area of the turbine which in Gorlov helical turbine that we have chosen has  $0.0081 \text{ m}^2$ .

## 2.7 Status of research work done on helical turbine

Tuyen Quang Le *et al* (14), studied the simulation of a flow driven rotor with a given load and analysed the operational characteristics of a vertical axis Darieus turbine i.e. it's self starting ability and fluctuations in torque and rotation per minute(RPM). It's been showed that the simulation of a flow driven rotor with a two dimensional turbine model had a power coefficients ( $C_p$ ) curves similar to those obtained in 3D simulation when a given tip speed ratio is less than one. 3D flow driven rotor simulation also showed that a helical blade turbine has the following advantages over a straight blade turbine of the same size i.e. Improvement in self starting capabilities and fluctuation reduction in its torque and increase in its power coefficient ( $C_p$ ) from 33% to 42%.

Dibakara Reddy *et al* (6) worked to prove that mild steel material can be used to make wind turbines which would provides strength and desired output. The aspect ratio i.e (H/D) and overlap ratio are taken for a savonius rotor wind turbine whose values were mentioned in the research paper (15). The design is done using CREO 2.0 and CFD analysis is performed using ansys 15.0. CFD analysis shows that all types of pressure calculations i.e static, dynamic and total etc came to be less than the material maximum value i.e  $3.5 \times 10^8 \text{ Pa}$  and thus it was shown that a savonius turbines made of mild steel can be used as they can provide strength as well as good power output.

Adam L Niblick *et al*<sup>(1)</sup>, studied the feasibility of a micro scale tidal hydrokinetic generator by giving more emphasis on turbine design. A model for a current velocity of 1.5 m/s is selected. Among several turbine designs he had chosen a helical cross-flow turbine, due to its self starting capability and its ability to accept flow from any direction. Parameters such as blade profile, aspect ratio, and helical pitch, number of blades, solidity ratio, and shaft diameter were selected for turbine. Three prototypes (two 3 bladed designs, with 15% and 30% solidity, and a 4 bladed design with 30% solidity and higher helical pitch) were fabricated and tested in a water flume having flow rates up to 0.8 m/s. It was analysed that a 4 bladed turbine with 60° helical pitch, 30% solidity, and circular plate “end cap” provided the best performance. This design attained the power coefficient of 24% in 0.8 m/s flow and experienced smaller efficiency reductions for tilted orientations as compared to other variants. It was shown that turbine efficiency increased with increased flume velocity. Model shows experimental trends as same but deviation occurs for some conditions which show that there is need to study of secondary effects due to chord to radius ratio of the turbine.

Himanshu Joshi *et al*<sup>(8)</sup>, designed and analysed the cross flow hydrokinetic helical blades. Analysis with optimum angular velocity<sup>(17)</sup> and constant pressure conditions<sup>(17)</sup> was performed for the blade with fixed pitch<sup>(17)</sup> by using Computational Fluid Dynamics (CFD) in fluent version 14.5 and Catia version 5 was used to carry out 3D modelling of the turbine. The hydrofoil shape of NACA 0018 was created by the airfoil coordinate data. Two different turbulence models Spalart Allmaras (a One Equation model) and sst k (a Two Equation model) were used to compute and compare the results. Profiles of drag and lift coefficients were calculated under a steady state flow of 1.5 m/s.

A. Reza Hassanzadeh *et al*<sup>(3)</sup>, studied a specific type of vertical axis turbine, called Savonius, appropriate for shallow water and low current velocity applications. Considering the low efficiency of Savonius, studies for enhancing the performance of Savonius utilization were carried out using CFD. Powerful computational fluid dynamic software was used to analyze and compare conventional turbine and helical turbine. The standard k epsilon turbulence model was used. The simulation results showed that the performance of helical Savonius rotor was significantly higher than conventional ones and showed the helical turbine does not create negative torque in comparison to the conventional turbine.

Andrea Alaimo *et al*<sup>(2)</sup>, analyzed the effects of mesh size and structure, time step and rotational velocity on performance of a straight blade vertical axis wind turbine and a helical

blade one. Analysis was carried out by using computational fluid dynamic ANSYS Fluent software. At first 2D simulations and then 3D simulations were carried to determine the performance parameters associated with the straight and helical blade turbines. The results were reported by varying the values of angular velocity. 2D simulation data have been collected at different tip speed ratio values and the result shows the torque, lift and drag coefficient behaviour of the rotor blade over a revolution with respect to its position. Subsequently, 3D analysis for four configurations i.e helix angle  $0^\circ$ ,  $30^\circ$ ,  $60^\circ$ ,  $90^\circ$ , has been performed. From simulations it has been observed that the helical blade has an average torque coefficient increased to 8.75% as compared to straight helical blade. Further, it has been shown that the generation of the tip vortices reduces the performance of Straight blade turbine. However 3D comparison shows that this effect is less prevalent in Helical VAWT as compared to straight one the Straight one.

Bachu Deb et al<sup>(4)</sup> analysed the performance of Savonius rotor two buckets bade by varying twisting angle from  $0^\circ$  to  $315^\circ$  with a step of  $45^\circ$ . A 3D Computational Fluid Dynamics analysis using Fluent 6.2 software was used to predict the performance of it without shaft and with end plates. A 2 bucket helical Savonius rotor model had a height of 60 cm and diameter 17 cm. k- $\epsilon$  model was used for calculation with standard wall condition. Power coefficients ( $C_p$ ) and torque coefficients ( $C_t$ ) at different tip speed ratios were analysed at different rotor angles. From the investigation, it was observed that power coefficient increased with increase of tip speed ratio up to an optimum limit, but then decreased even further tip speed ratio was increased. It has been shown that performance of turbine becomes maximum when angle of rotation is  $45^\circ$  and  $225^\circ$ .

MD. Saddam Hussen *et al*<sup>[11]</sup> studied the behaviour and performance of NACA 0018 three bladed vertical axis wind turbine rotor. Straight blades were twisted to  $45^\circ$  and  $90^\circ$  in order to improve the performance of rotor. By twisting the rotor and maintaining the height and diameter of rotors, the weight of rotor was significantly increased. Therefore, to decrease the weight without compromising the performance of the rotor blade, the fibre reinforced composite materials are used. This was fabricated from carbon, glass fibres, and epoxy resin which were used to increase the strength to weight ratio. Analysis was carried out in Ansys. It showed the following results of static and dynamic pressure for straight blade,  $45^\circ$  twisted blades and  $90^\circ$  twisted blades.

Md. Intiaj Hassan *et al* <sup>[9]</sup> analysed a 180° Twisted Savonius rotor having two end plates using computational fluid dynamics. 3D Simulations flows were performed in CFD software, using RANSE solver with rectangular mesh. The proposed rotor has 180° twist with two end plates with circular central shaft and has a height of 0.32m and a diameter of 0.2286m. Performance of the twisted Savonius rotor was analysed using starting characteristics i.e. inlet velocity, static torque and angular velocity of the turbine. Simulation results showed better performance for twisted Savonius rotor as compared to conventional Savonius rotors. Designed twisted rotor will be used in a small power generation system. This paper showed that CFD can be used to study the behaviour of water current turbine. In future the prototype will be made to compare the CFD results and experimental results. The main objective is to develop a simulation model of the turbine that can replace expensive experimental setup.

Travis E. Salyers <sup>[13]</sup>, analyzed six different rotor designs with equal swept areas using wind tunnel and numerical method. First model is a conventional Savonius with 2 blades, second model named “CC” model, third model named “QM” model, and fourth, fifth and sixth model is a 90 degree helical twist models with 2, 3, and 4 blades respectively. Open type wind tunnel was used to calculate RPM and torque over a varying range of wind speeds. For numerical approach, ANSYS Fluent simulations were used, Models were designed using Solid Works. CC and QM cross-sections shows reduce negative torque on the blades by 20 degrees as compared to first Savonius model. Helical designs showed positive torque over all operational angles. Helical models with 2 and 3 blades have shown best self-starting capability at low wind speeds. Under no loading conditions, Helical 3 shows 35 RPM at 1.4 m/s wind velocity. The highest power coefficient (C<sub>p</sub>) in the study is achieved by the helical VAWT 2 blades both experimentally and numerically.

Mr.Laxmikant *et al* <sup>[10]</sup> presented its review on performance and testing methodology of savonius VAWT. Savonius wind turbine has a poor efficiency. Many researchers proposed different configuration to increase its efficiency. In this paper they took various factors such as aspect ratio, overlap ratio, number of blade, interference of shaft, influence of velocity, shape of rotor and how by varying these parameters performance of turbine can be increased. Numerical method using software provides good result as compared to experimental method as less expensive and less time consuming. Numerous configurations were used to enhance the performance of savonius wind turbine.



## Chapter 3 METHODOLOGY

### 3.1 Introduction

Performance studies were conducted by creating a mathematical (CFD) model of the helical turbine using ANSYS 15.0 software. The mathematical model so formulated was subjected to simulation studies. The initial dimensions of the model were in accordance with that of the laboratory model of helical turbine used by Gorlov <sup>[15]</sup> (Table 3.1).

**Table 3.1** Gorlov Helical turbine dimensions

Specification	Parameter value
Turbine diameter	24 inch
Turbine length (height)	34 inch
Hydrofoil shape	NACA 0020 - 7 inch chord
No. of blades	3
Helix angle	120 <sup>0</sup>
Upper and lower plate thickness (circular in shape)	1 cm

#### 3.1.1 Ansys fluent:

Ansys is software platform which offers a comprehensive software tools that spans the entire range of physics, providing access to virtually any field of engineering simulation that a design process requires. Fluent is one of its tools, which is based on computational fluid dynamics for calculation of complex flow in various fields of fluid dynamics. It has been widely used by researchers in aerodynamics fields and now in the fields of hydraulics and hydrology also it is gaining momentum. Ansys fluent allows us to choose one of the two numerical methods:

- 1) pressure-based solver
- 2) density-based solver

The pressure-based approach was developed for low-speed incompressible flows, while the density-based approach was mainly used for high-speed compressible flows. However, recently both methods have been extended and reformulated to solve and operate for a wide range of flow conditions beyond their traditional or original intent. In both methods the velocity field is obtained from the momentum equations. In the density-based approach, the

continuity equation is used to obtain the density field while the pressure field is determined from the equation of state. On the other hand, in the pressure-based approach, the pressure field is extracted by solving a pressure or pressure correction equation which is obtained by manipulating continuity and momentum equations. Using either method, ansys fluent will solve the governing integral equations for the conservation of mass and momentum, and (when appropriate) for energy and other scalars such as turbulence and chemical species. In both cases a “control-volume-based technique” is used that consists of:

- 1) Division of the domain into discrete control volumes using a computational grid.
- 2) Integration of the governing equations on the individual control volumes to construct algebraic equations for the discrete dependent variables ("unknowns") such as velocities, pressure, temperature, and conserved scalars.
- 3) Linearization of the discretized equations and solution of the resultant linear equation system to yield updated values of the dependent variables

### 3.1.2 Hydrofoil coordinates:

In the term NACA-0020, NACA stand for national advisory committee for aeronautics, in 0020 the first two 00 shows that the camber line slope is zero and the hydrofoil is not the curved one as shown in figure 3.2 and 3.3. camber line is the line that pass through the middle of the foil from its head to tail, 20 defines the % thickness w.r.t to chord length. Drawing detailing of hydrofoil has been shown in figure 3.1. NACA 0020 coordinates were obtained and got converted into 7 inch chord whose table has been shown below as table 3.2 and then imported in design modeller, firstly the design of hydrofoil was made using spline curve but since ansys 15.0 could not mesh the spline curve model therefore its hydrofoil shape was made using various arc as shown in fig 3.3 and 3.4

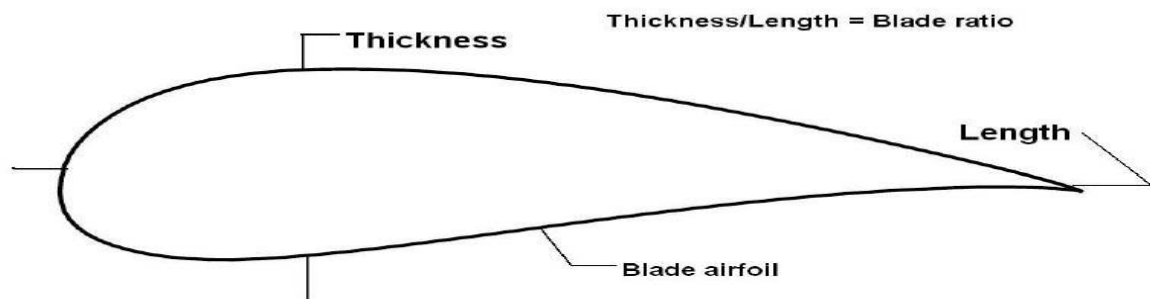


**Figure 3.1** Foil details

Three such hydrofoils are made so as to have helix angle of  $120^{\circ}$  as shown in figure 3.5. With three hydrofoils and helix angle of  $120^{\circ}$  Gorlov helical turbine becomes fully submerged so has to have a constant torque throughout its operation. By increasing the helix angle of the blades, turbine would be designed for partial submerged conditions, like for  $150^{\circ}$  it would be for  $3/4^{\text{th}}$  submerged condition and for  $180^{\circ}$  it would be operational for half submerged flow. If helix angle is decreased then even in fully submerged condition there will be fluctuation in torque produced.

**Table 3.2** NACA-0020 coordinate table for 7 inch chord

Plane no.	Serial no. of a point	X coordinate	Y coordinate	Z coordinate
1	1	17.75000	0	0
1	2	17.74221	0.001882	0
1	3	17.71887	0.007526	0
1	4	17.68001	0.016916	0
1	5	17.62571	0.02998	0
1	6	17.55606	0.046647	0
1	7	17.47118	0.066864	0
1	8	17.37122	0.090507	0
1	9	17.25634	0.11747	0
1	10	17.12676	0.147609	0
1	11	16.98272	0.180802	0
1	12	16.82444	0.216887	0
1	13	16.65222	0.255689	0
1	14	16.46636	0.297046	0
1	15	16.26718	0.340765	0
1	16	16.05502	0.386684	0
1	17	15.83028	0.434591	0
1	18	15.59334	0.484309	0
1	19	15.34459	0.535624	0
1	20	15.08452	0.588359	0
1	21	14.81353	0.642302	0
1	22	14.53214	0.697256	0

1	23	14.24083	0.753008	0
1	24	13.94009	0.809382	0
1	25	13.63046	0.866165	0
1	26	13.31250	0.923124	0
1	27	12.98675	0.980102	0
1	28	12.65380	1.036831	0
1	29	12.31420	1.093152	0
1	30	11.96858	1.148833	0
1	31	11.61752	1.203628	0
1	32	11.26167	1.257357	0
1	33	10.90161	1.309755	0
1	34	10.53802	1.360609	0
1	35	10.17150	1.40967	0
1	36	9.802686	1.456707	0
1	37	9.432261	1.501473	0
1	38	9.060860	1.543718	0
1	39	8.689140	1.583194	0
1	40	8.317739	1.61967	0
1	41	7.947314	1.65288	0
1	42	7.578505	1.682594	0
1	43	7.211985	1.70858	0
1	44	6.848394	1.73059	0
1	45	6.488335	1.748428	0
1	46	6.132483	1.761883	0
1	47	5.781424	1.770776	0
1	48	5.435796	1.774911	0
1	49	5.096203	1.774148	0
1	50	4.763248	1.768379	0
1	51	4.437500	1.757463	0
1	52	4.119544	1.741364	0
1	53	3.809913	1.719975	0
1	54	3.509175	1.693315	0

1	55	3.217862	1.661365	0
1	56	2.936471	1.624161	0
1	57	2.665482	1.581756	0
1	58	2.405409	1.534257	0
1	59	2.156661	1.481735	0
1	60	1.919716	1.424367	0
1	61	1.694983	1.362277	0
1	62	1.482817	1.295661	0
1	63	1.283645	1.224679	0
1	64	1.097784	1.149561	0
1	65	0.925556	1.07052	0
1	66	0.767279	0.987752	0
1	67	0.623238	0.901487	0
1	68	0.493663	0.811938	0
1	69	0.378785	0.719337	0
1	70	0.278817	0.623859	0
1	71	0.193937	0.525684	0
1	72	0.124286	0.425024	0
1	73	0.069988	0.321985	0
1	74	0.031134	0.216745	0
1	75	0.007792	0.109376	0
1	76	0.000000	0	0
1	77	0.007792	-0.10938	0
1	78	0.031134	-0.21675	0
1	79	0.069988	-0.32199	0
1	80	0.124286	-0.42502	0
1	81	0.193937	-0.52568	0
1	82	0.278817	-0.62386	0
1	83	0.378785	-0.71934	0
1	84	0.493663	-0.81194	0
1	85	0.623238	-0.90149	0
1	86	0.767279	-0.98775	0

1	87	0.925556	-1.07052	0
1	88	1.097784	-1.14956	0
1	89	1.283645	-1.22468	0
1	90	1.482817	-1.29566	0
1	91	1.694983	-1.36228	0
1	92	1.919716	-1.42437	0
1	93	2.156661	-1.48173	0
1	94	2.405409	-1.53426	0
1	95	2.665482	-1.58176	0
1	96	2.936471	-1.62416	0
1	97	3.217862	-1.66136	0
1	98	3.509175	-1.69331	0
1	99	3.809913	-1.71998	0
1	100	4.119544	-1.74136	0
1	101	4.437500	-1.75746	0
1	102	4.763248	-1.76838	0
1	103	5.096203	-1.77415	0
1	104	5.435796	-1.77491	0
1	105	5.781424	-1.77078	0
1	106	6.132483	-1.76188	0
1	107	6.488335	-1.74843	0
1	108	6.848394	-1.73059	0
1	109	7.211985	-1.70858	0
1	110	7.578505	-1.68259	0
1	111	7.947314	-1.65288	0
1	112	8.317739	-1.61967	0
1	113	8.689140	-1.58319	0
1	114	9.060860	-1.54372	0
1	115	9.432261	-1.50147	0
1	116	9.802686	-1.45671	0
1	117	10.17150	-1.40967	0
1	118	10.53802	-1.36061	0

1	119	10.90161	-1.30975	0
1	120	11.26167	-1.25736	0
1	121	11.61752	-0.98674	0
1	122	11.96858	-1.14883	0
1	123	12.31420	-1.09315	0
1	124	12.65380	-1.03683	0
1	125	12.98675	-0.9801	0
1	126	13.31250	-0.92312	0
1	127	13.63046	-0.86616	0
1	128	13.94009	-0.80938	0
1	129	14.24083	-0.75301	0
1	130	14.53214	-0.69726	0
1	131	14.81353	-0.6423	0
1	132	15.08452	-0.58836	0
1	133	15.34459	-0.53562	0
1	134	15.59334	-0.48431	0
1	135	15.83028	-0.43459	0
1	136	16.05502	-0.38668	0
1	137	16.26718	-0.34076	0
1	138	16.46636	-0.29705	0
1	139	16.65222	-0.25569	0
1	140	16.98272	0.216887	0
1	141	17.12676	-0.1808	0
1	142	17.25634	-0.14761	0
1	143	17.37122	-0.11747	0
1	144	17.47118	-0.09051	0
1	145	17.55606	-0.06686	0
1	146	17.62571	-0.04665	0
1	147	17.68001	-0.02998	0
1	148	17.71887	-0.01692	0
1	149	17.74221	-0.00753	0
1	150	17.75000	-0.00188	0

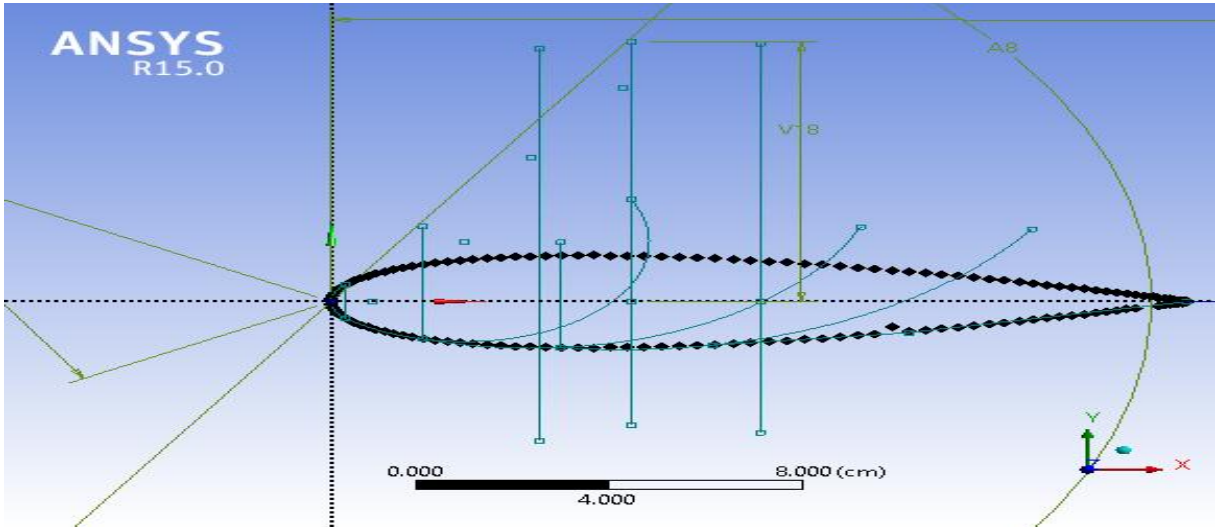


**Figure 3.2** Drawing detailing of hydrofoil

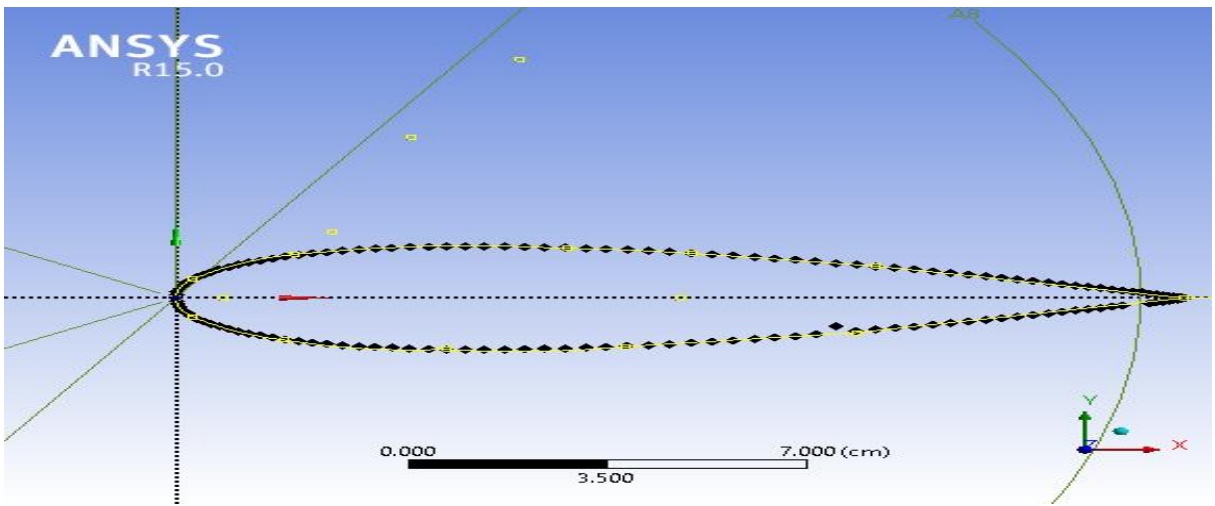


**Figure 3.3** Hydrofoil coordinates sketch

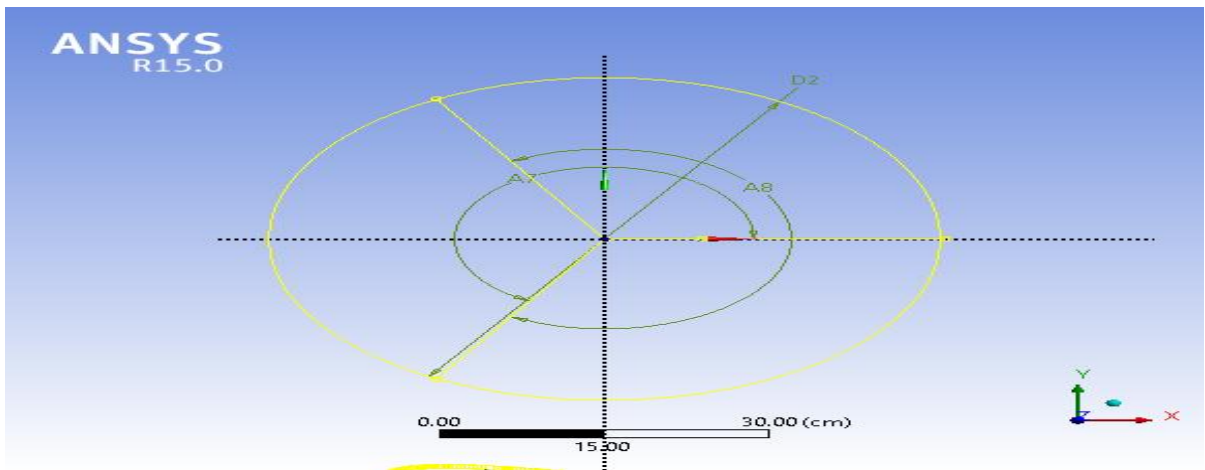


**Figure 3.4** Base plate sketch



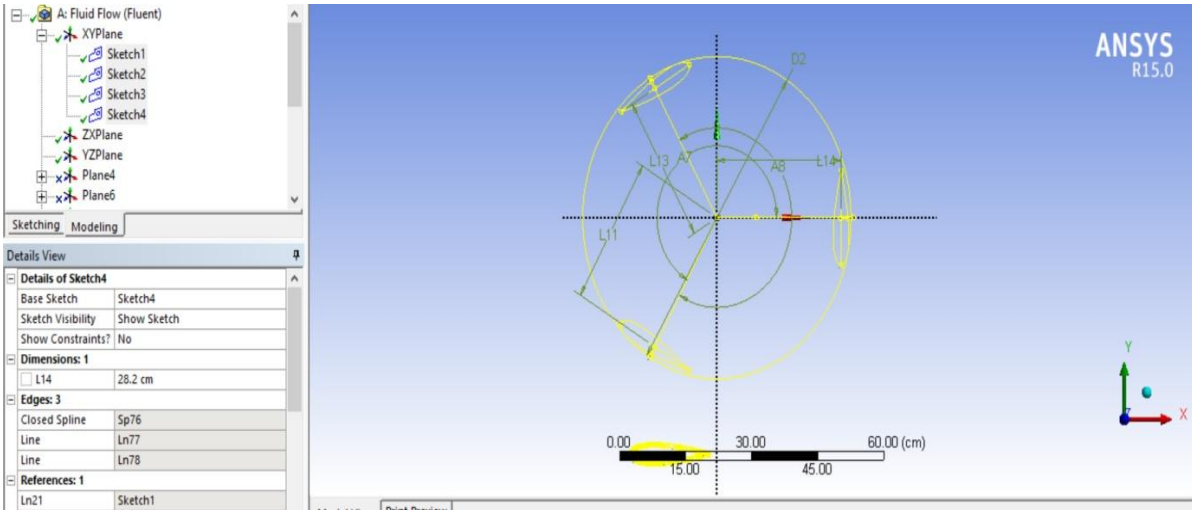


**Figure 3.5** Base plate sketch with hydrofoil

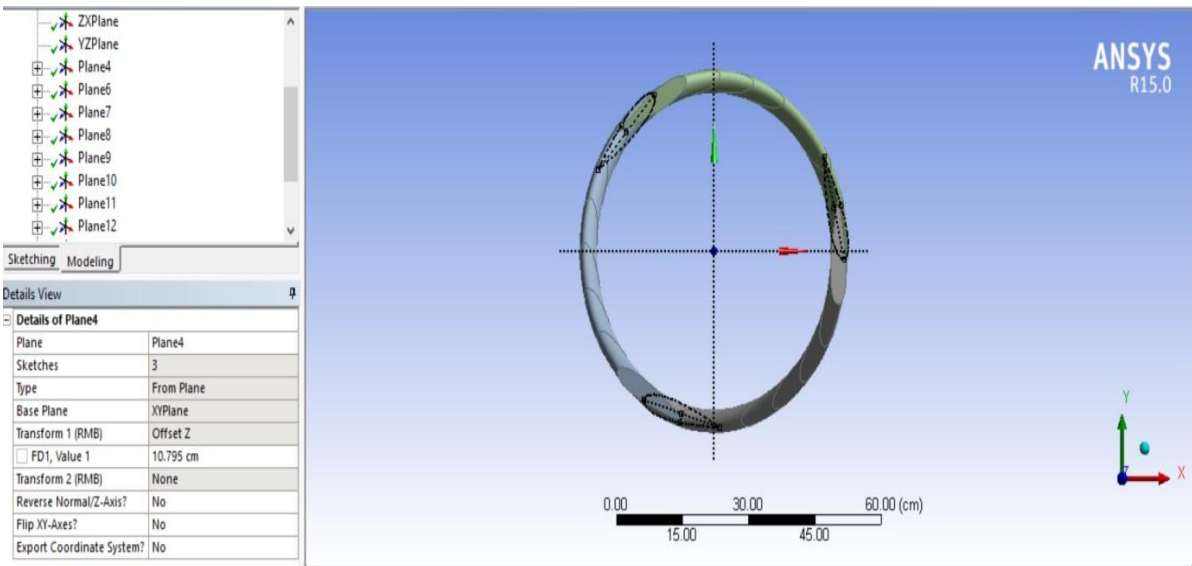


**Figure 3.6** Plan of swept model of helical blades

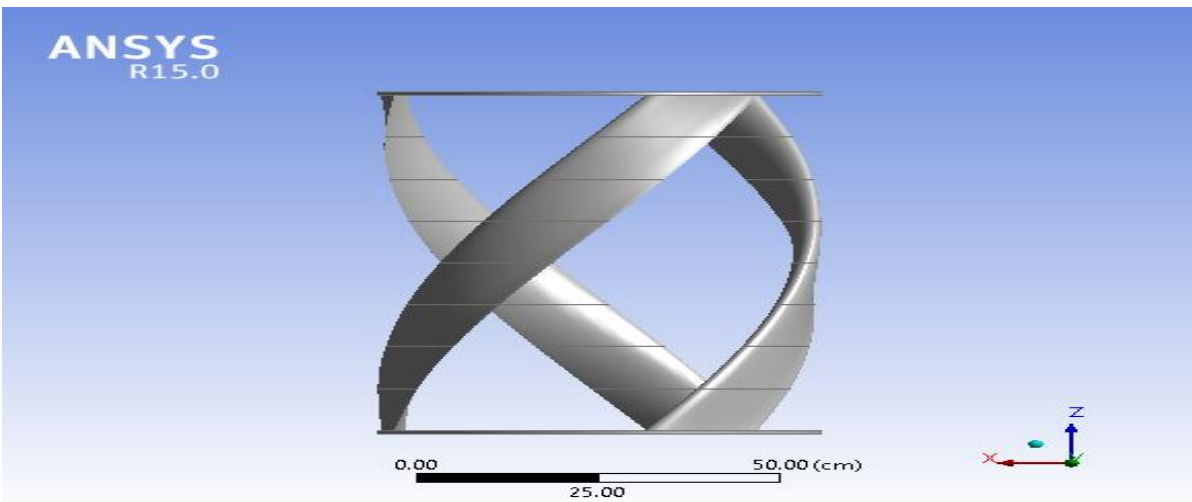


**Figure 3.7** Elevation of swept model of helical blades

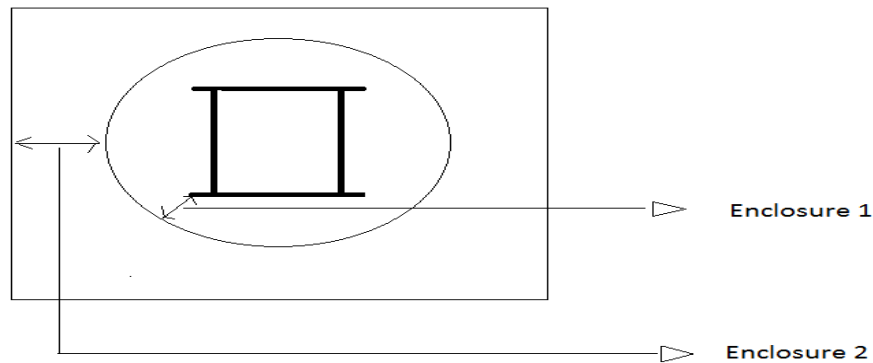


**Figure 3.8** Enclosure detailing

Enclosure 1 was taken as .04m whereas enclosure 2 was taken as 0.4315m so as to have a channel cross section of 2m x 2m sides. Enclosures are fluid domain regions where enclosure 1 denotes the region around the turbine in which fluid particles rotates due to inertia of the rotational motion of the turbine whereas enclosure 2 domain gives the channel cross section domain. On calculation both the region gets clubbed by using option “copy to mesh motion” when calculation is done on transient conditions.

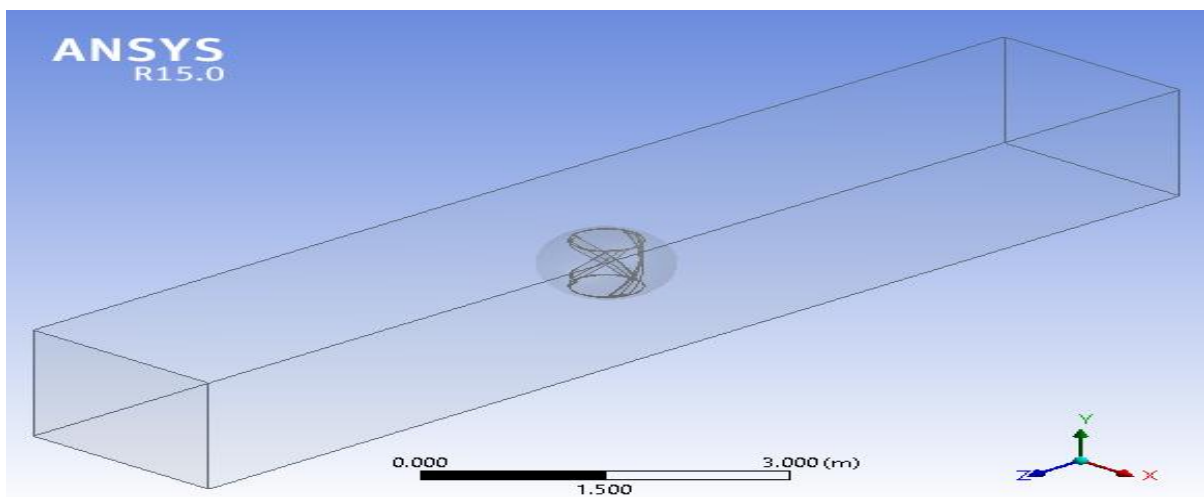


**Figure 3.9** Turbine model with enclosures

### 3.2 Discretization.

In Ansys fluent domain is discretized into a finite set of control volumes technique. Method of relevance centre is chosen for meshing and is taken as fine since in coarse it was showing a failed meshed region with total no of nodes as 208062 and no. of elements as 1150311. To

give computational domain a begin and end for calculation, create named selection is used therefore from Create named selection inlet, outlet sections, wall faces are provided as shown in fig 3.11,3.12 and 3.13 respectively. In figure 3.13 all the faces are taken as wall since this turbine is designed for fully submerged condition, for partial submerged condition upper face would be taken as ‘symmetry’ one.

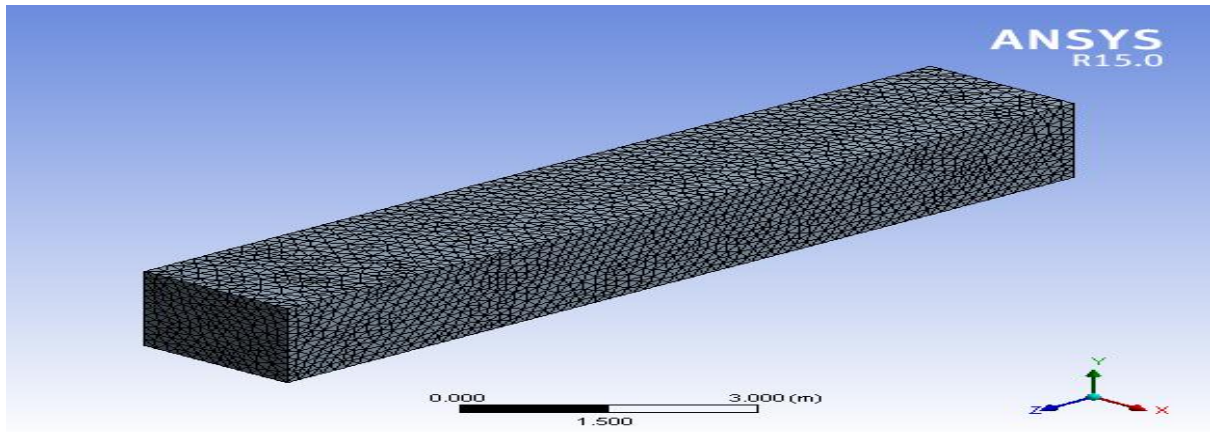


**Figure 3.10** Mesh figure

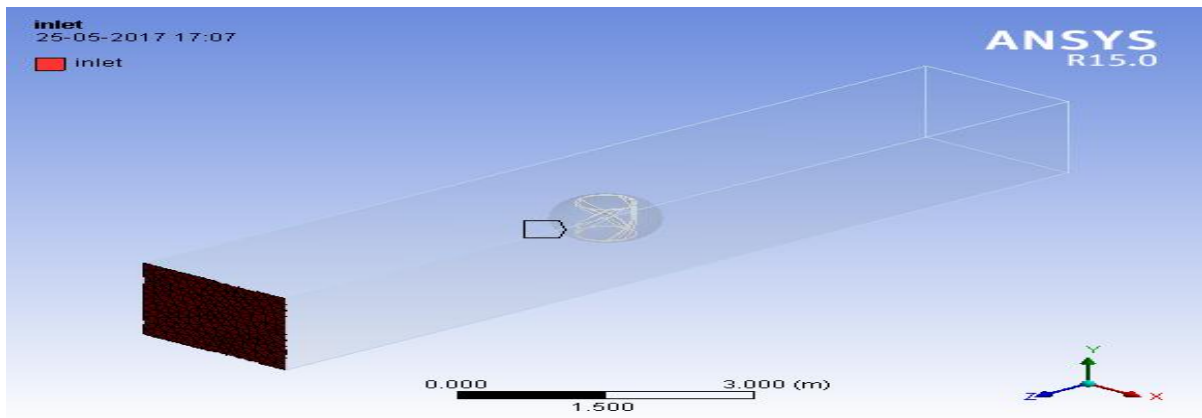


**Figure 3.11** Inlet section

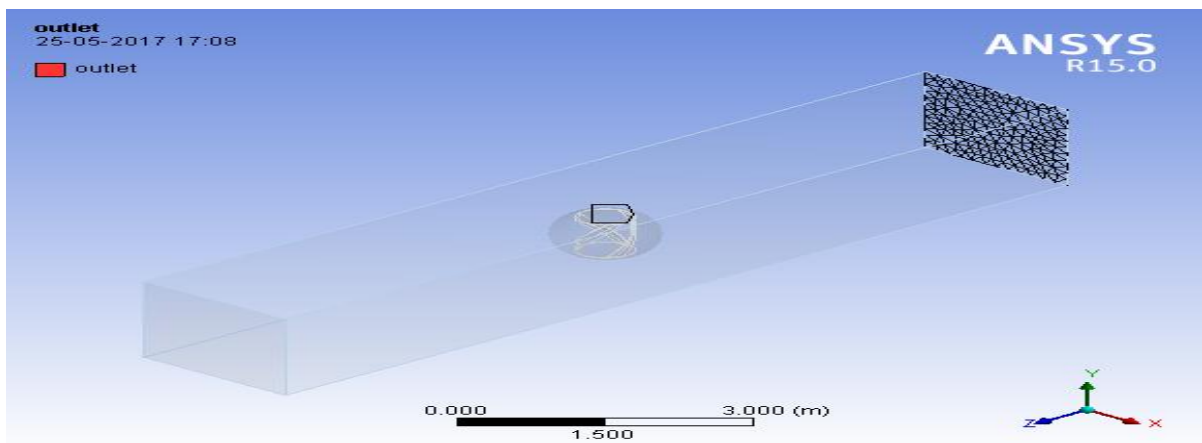


**Figure 3.12** Outlet section

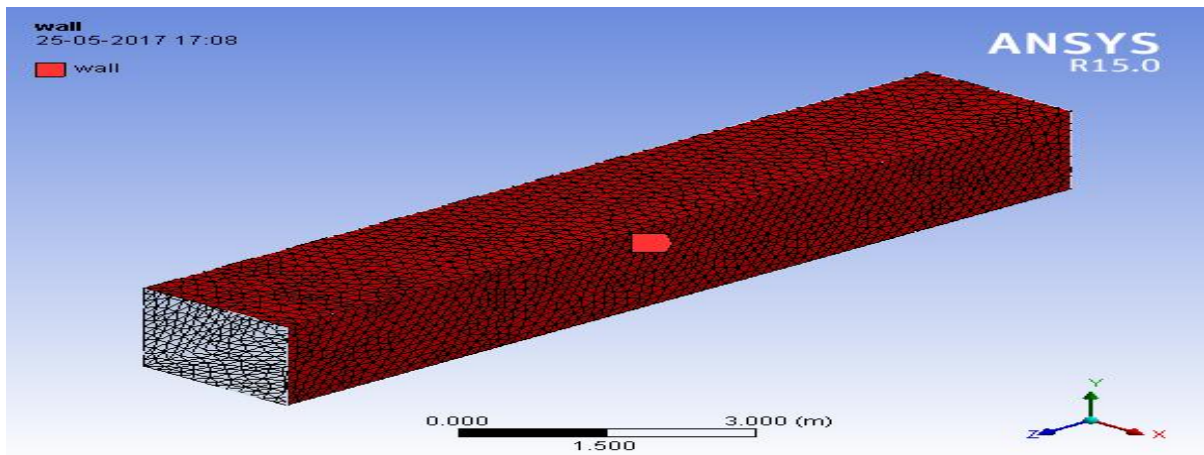


**Figure 3.13** Wall section

### 3.3 Governing equation:

In the laminar regime, the flow of the fluid can be completely predicted by solving the steady-state Navier-Stokes equations, which predict the velocity and the pressure fields. We can assume that the velocity field does not vary with time and get an accurate prediction of the flow behaviour. As the flow begins to transition to turbulence, chaotic oscillations appear in the flow and it is no longer possible to assume that the flow is invariant with time. In this case, it is necessary to solve the problem in the time domain, and the mesh used must be fine enough to resolve the size of the smallest eddies in the flow. As the Reynolds number increases, the flow field exhibits small eddies and the timescales of the oscillations become so short that it is computationally unfeasible to solve the Navier-Stokes equations. In this flow regime, we can use a Reynolds-averaged Navier-Stokes (RANS) formulation, which is based on the observation that the flow field over time contains small and local oscillations. The objective of the turbulence models for the RANS equations is to compute the Reynolds stresses which can be done by three main categories of RANS-based turbulence models as Linear eddy viscosity models, Nonlinear eddy viscosity models, Reynolds stress model (RSM). Of these we will discuss about linear eddy viscosity models which there are of three types as Zero equation model, One equation model, Two equation model. Zero-equation turbulence models are models that do not require the solution of any additional equations, and are calculated directly from the flow variables. As a consequence, zero equation models may not be able to properly account for history effects on the turbulence, such as convection and diffusion of turbulent energy. These models are often too simple for use in general situations, but can be quite useful for simpler flow geometries or in start-up situations (e.g. the initial phases of a computation in which a more complicated model may have difficulties). The two most well known zero equation models are:

1) Baldwin-Lomax model: It is a two-layer algebraic zero equation model which gives the eddy viscosity as a function of the local boundary layer velocity profile. The model is suitable for high-speed flows with thin attached boundary-layers, typically present in aerospace and turbo machinery applications

2) Cebeci-Smith model: It is a zero equation eddy viscosity model used in computational fluid dynamics analysis of turbulent boundary layer flows. The model gives eddy viscosity,  $\mu_t$ , as a function of the local boundary layer velocity profile

One equation turbulence models solve one turbulent transport equation, usually the turbulent kinetic energy. The original one-equation model is Prandtl's one-equation model. Other common one-equation models are:

1) Baldwin-Barth model: modification is done by replacing the  $y$  dependent near wall formulation with equivalent functions based on the ratio of the large eddy and the Kolmogorov time scales

2) Spalart Allmaras model: Spalart Allmaras model is a one equation model which solves a transport equation for a viscosity

Two equation turbulence models are one of the most common types of turbulence models. Models like the  $k$ -epsilon model and the  $k$ -omega model have become industry standard models and are commonly used for most types of engineering problems. Two equation turbulence models are also very much still an active area of research and new refined two-equation models are still being developed. By definition, two equation models include two extra transport equations to represent the turbulent properties of the flow. This allows a two equation model to account for history effects like convection and diffusion of turbulent energy. The three two equation models are:

1)  $k$ -epsilon models: It includes two extra transport equations to represent the turbulent properties of the flow.

a) Standard  $k$ -epsilon model: It is the also a basic  $K$ -epsilon model. Later on modification were done on this model to get the next  $K$ -epsilon models.

b) Realisable  $k$ -epsilon model: It is an improvement over the standard  $k$ - $\epsilon$  model and is a well-established model capable of resolving through the boundary layer.

c) RNG  $k$ -epsilon model: This was developed using Re-Normalisation Group (RNG) methods by Yakhot et al to renormalize the Navier-Stokes equations, to account for the effects of smaller scales of motion.

d) Near-wall treatment: is a blended wall model or wall function. It blends the separate models in the two-layer approach by use of a damping function so that the transition between the two is smoother.

2) k-omega models: Here k determines the energy in the turbulence and  $\omega$ , the specific dissipation determines the scale of the turbulence.

a) SST k-omega model: It is a two-equation eddy-viscosity model. Shear stress transport (SST) in the inner parts of the boundary layer makes the model directly usable all the way down to the wall through the viscous sublayer, hence the SST k- $\omega$  model can be used as a Low-Re turbulence model without any extra damping functions

b) Near-wall treatment: It is again a blended wall model as it blends the separate models in the two layer approach by damping function so that the transition between the two is smoother.

We use two equation models because they are simplest and complete models in which the solution of two separate transport equations allows the turbulent velocity and length scales to be independently determined. Out of these k- $\epsilon$  model is used more because Basic assumption in this model is that the turbulent viscosity is isotropic i.e. The ratio between Reynolds stress and mean rate of deformations is the same in all direction. Initially standard k- $\epsilon$  model was in use but later on improvements have been made to the model to improve its performance. Three of its variants are available realizable, RNG and enhanced wall treatment. For practical approach, the standard k- $\epsilon$  turbulence model (by Launder and Spalding, 1974) is used where unknowns are minimized and which can be applied to a large number of turbulent applications. The turbulence kinetic energy k and its rate of dissipation  $\epsilon$  in k- $\epsilon$  model are obtained from the following transport equations:

$$\frac{\partial(\rho k)}{\partial t} + \frac{\partial}{\partial x_i}(\rho k u_i) = \frac{\partial}{\partial x_j} \left[ \mu + \frac{\mu_t}{\sigma_k} \right] \left[ \frac{\partial k}{\partial x_j} \right] + G_k + G_b - \rho \epsilon - Y_M + S_k \quad \dots 3.1$$

And

$$\frac{\partial(\rho \epsilon)}{\partial t} + \frac{\partial}{\partial x_i}(\rho \epsilon u_i) = \frac{\partial}{\partial x_j} \left[ \mu + \frac{\mu_t}{\sigma_k} \right] \left[ \frac{\partial \epsilon}{\partial x_j} \right] + C_{1\epsilon} \frac{\epsilon}{k} (G_k + C_{3\epsilon} G_b) - C_{2\epsilon} \rho \frac{\epsilon^2}{k} + S_\epsilon \quad \dots 3.2$$

In these equations,  $u_i$  represent velocity component in corresponding direction.  $G_k$  represents the generation of turbulence kinetic energy due to the mean velocity gradients,  $G_b$  is the generation of turbulence kinetic energy due to buoyancy,  $Y_M$  represents the contribution of the fluctuating dilatation in compressible turbulence to the overall dissipation rate.  $C_{1\epsilon}$ ,  $C_{2\epsilon}$

and  $C_{3\varepsilon}$  are constants.  $\sigma_k$  and  $\sigma_\varepsilon$  are the turbulent Prandtl numbers for  $k$  and  $\varepsilon$ , respectively.  $S_k$  and  $S_\varepsilon$  are user-defined source terms.

$$\mu_t = \rho C_\mu \frac{k^2}{\varepsilon}$$

The values of constants have been derived by numerous iterations of data fitting for a wide range of turbulent flows. These are as follows:

$$C_\mu = 0.09 \quad \sigma_k = 1.00 \quad \sigma_\varepsilon = 1.30 \quad C_{1\varepsilon} = 1.44 \quad C_{2\varepsilon} = 1.92$$

In Ansys fluent domain is discretized into a finite set of control volumes and above equation are solved on this set of control volumes

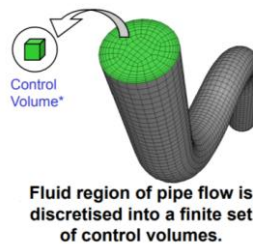


**Figure 3.14** Control volume discretization.

Fluent control volumes are cell-centred (i.e. they correspond directly with the mesh) .As far as the residuals are concerned the residuals software tells nothing about the accuracy of the solution. If they are decreasing, then it only shows that the flow is changing less and less as iteration proceeds, which means it is converging. To monitor convergence, flow parameters are monitored in addition to the residuals. For a steady state solution, the net mass flow rate at the boundaries can be monitored. For a steady flow, this should be zero (or close to it, due to round-off). If the lift coefficient is required to be monitored, then it is monitored. When it converges, it means one can stop the simulation as it will no longer give a different answer for that particular parameter.

### 3.4. Calculation of $C_L$ , $C_D$ and $C_m$ :

Since from CFD we can find the variable such as velocity, pressure etc at any point in the fluid domain. Now since when the fluid flows over a foil it produces a lift and drag force on the foil from where the software calculates the value of  $C_D$  and  $C_L$ . The lifting force acting on a body in a fluid flow can be calculated

$$F_L = 1/2 C_L \rho V^2 A \quad \dots 3.3$$

Where

$F_L$  = lifting force (N)

$C_L$  = lifting coefficient

$\rho$  = density of fluid ( $\text{kg/m}^3$ )

$V$  = flow velocity (m/s)

$A$  = body area ( $\text{m}^2$ ) (here it is swept area of a hydrofoil)

And the drag force acting on a body in fluid flow can be calculated

$$F_D = 1/2 C_D \rho V^2 A \quad \dots 3.4$$

Where

$F_D$  = drag force (N)

$C_D$  = drag coefficient

$\rho$  = density of fluid ( $\text{kg/m}^3$ )

$V$  = flow velocity (m/s)

$A$  = body area ( $\text{m}^2$ )

Now in the paragraph 2.5 it has been written that their yields an apparent flow on rotation, which produces two orthogonal vectors as a radial component and a tangential component, shown here as “Normal force” and “Axial force” respectively. Of these the remaining force component i.e. the tangential component propels the turbine in the clockwise direction, and it is from this the torque (T) can be calculated which is force (F) multiplied by distance from the axis of rotation. When Force F is known, V,  $\rho$  and A is known then  $C_D$  and  $C_L$  can be calculated easily from equation 6 and 7 on one node which on integration over the whole swept area of the blade hydrofoil gives the value that we get as a result. Similarly when on a finite element Torque T is known, velocity V is known, D that is the diameter of the turbine or the distance of foil from the axis of rotation is known then  $C_m$  can be calculated from the equation no. 3. But since it has been calculated on one node therefore the result we got is the integrated result over the whole swept area of the hydrofoil of the turbine.

### 3.5 Boundary conditions:

Boundary conditions are taken as follows:

**Table 3.3** Boundary Conditions

S.no	Boundary	Boundary condition
1	Inlet	Inlet velocity = 1.5m/s, gauge pressure as 0 Pascal



2	outlet	Gauge pressure as 0 Pascal
3	Slip condition at side, bottom and upper wall	Hydro dynamically smooth boundary with no slip condition

Pressure solver is chosen since the fluid is water. Model chosen for calculation is k-ε standard wall function, angular velocity of sphere is taken as 100 rpm. No. of iterations for the convergence is set as 1000 under steady state conditions which were then taken as 144 iterations in transient conditions by taking time step size as 0.0016s.

Time step is calculated as follows:

$$\begin{aligned}
 100 \text{ rpm} &= 1.6666 \text{ rotation per second} \\
 &= 0.6002 \text{ second per rotation}
 \end{aligned}$$

Now if every rotation is divided into 36 equal parts then it is  $0.6002/36 = 0.0166$  s. so we will use 0.0166 s as time step to have more precise result.

## Chapter 4 RESULTS AND DISCUSSION

### 4.1. Model Validation

**Table 4.1** Validation table

Simulation result	Experimental result
<p>Since the value of <math>C_m</math> that comes out is 0.163420318 when enclosure 1 is 0.04 m and enclosure 2 is 0.4315 m and we know that power coefficient is written as</p> $C_p = \text{Tip Speed Ratio} \times \text{moment coefficient}$ $= (\omega D/2V) \times C_m$ <p>Where <math>\omega = 10.47 \text{ rad/s}</math> (100 rpm)</p> <p><math>D = 0.6096 \text{ m}</math> (24 inch)</p> <p><math>V = 1.5 \text{ m/s}</math> (5 ft/s)</p> <p><math>C_m = 0.163420318</math></p> <p>When we substitute the above values in equation 1 then its gives:</p> <p><b><math>C_p = 0.35</math></b></p>	<p>Experimentally by Gorlov on the models shows that at inlet velocity of 1.5 m/s, angular velocity of 100 rpm with swept area of 0.0081 square metres the efficiency of turbine comes out to be <b>35 %</b>.</p> <p>Which means <b><math>C_p</math> comes out to be as 0.35.</b></p>

Since enclosure 1 at 35 % efficiency is 0.04 m which means that fluid within the volume of a sphere of radius 0.5685 m from the centre of turbine is rotating with the turbine due to inertia caused by the rotational motion of the turbine.

### 4.2 Variation of $C_m$ with change in enclosures

We have taken the channel cross section dimensions as 2m x 2m. since initially enclosure 1 was taken as 0.4m therefore enclosure 2 is kept as 0.0715 to keep the channel cross section as 2m x 2m and its  $C_m$  value was found at wall-sphere which came out as 0.0469. Therefore

enclosure1 was varied and was found that  $C_m$  i.e moment coefficient increases, when enclosure1 decreases and subsequently enclosure 2 is increased to keep the channel cross section as 2m x 2m.

**Table 4.2** variation of  $C_m$  with change in enclosures

Radius of sphere of influence(m)	Box side (m)	Enclosure 1(sphere) (m)	Enclosure 2(box)(m)	$C_m$	$\lambda$	$C_p$	efficiency
0.5285+0.5	2	0.5	NA	...	2.12	...	...
0.5285+0.4	2	0.4	0.0715	0.0469	2.12	0.0994	9.9428
0.5285+0.3	2	0.3	0.1715	0.0512	2.12	0.1085	10.8544
0.5285+0.2	2	0.2	0.2715	0.0771	2.12	0.1634	16.3452
0.5285+0.1	2	0.1	0.3715	0.0976	2.12	0.2069	20.6912
0.5285+0.09	2	0.09	0.3815	0.0932	2.12	0.1975	19.7584
0.5285+0.08	2	0.08	0.3915	0.1004	2.12	0.2128	21.2848
0.5285+0.07	2	0.07	0.4015	0.1023	2.12	0.2168	21.6876
0.5285+0.06	2	0.06	0.4115	0.1415	2.12	0.2998	29.998
0.5285+0.05	2	0.05	0.4215	0.1605	2.12	0.3402	34.026
<b>0.5285+0.04</b>	<b>2</b>	<b>0.04</b>	<b>0.4315</b>	<b>0.1647</b>	<b>2.12</b>	<b>0.3491</b>	<b>34.9164</b>

In the figure 4.1 it has been shown that as the value of enclosure 1 is decreasing the value of moment coefficient starts increasing. Since at enclosure 1 as 0.04 m and enclosure 2 as 0.4315, the moment coefficient comes out to be 0.16 which gives the efficiency of the turbine as 35 % from where our result got validated with the Gorlov published data result <sup>[7]</sup> whose calculation has been shown in table 4.1. Therefore the same value of enclosure 1 and enclosure 2 is taken for every performance analysis on different design turbines. After 100 iterations moment coefficient ( $C_m$ ) value starts comes out to be in between 0.16 and 0.17 and which shows a constant trend thereby indicates a constant torque production by the helical turbine and the solution got converged at 444 iterations. Then a duplicate of the fluent project is generated where transient condition is taken and where time steps size was taken as 0.0016s and no of time steps were taken as 72. Since it was taking 450 iterations to get the converged results which was a time taking step as taking four to six hours for one complete result therefore we have taken 200 iterations only for different calculation procedure.

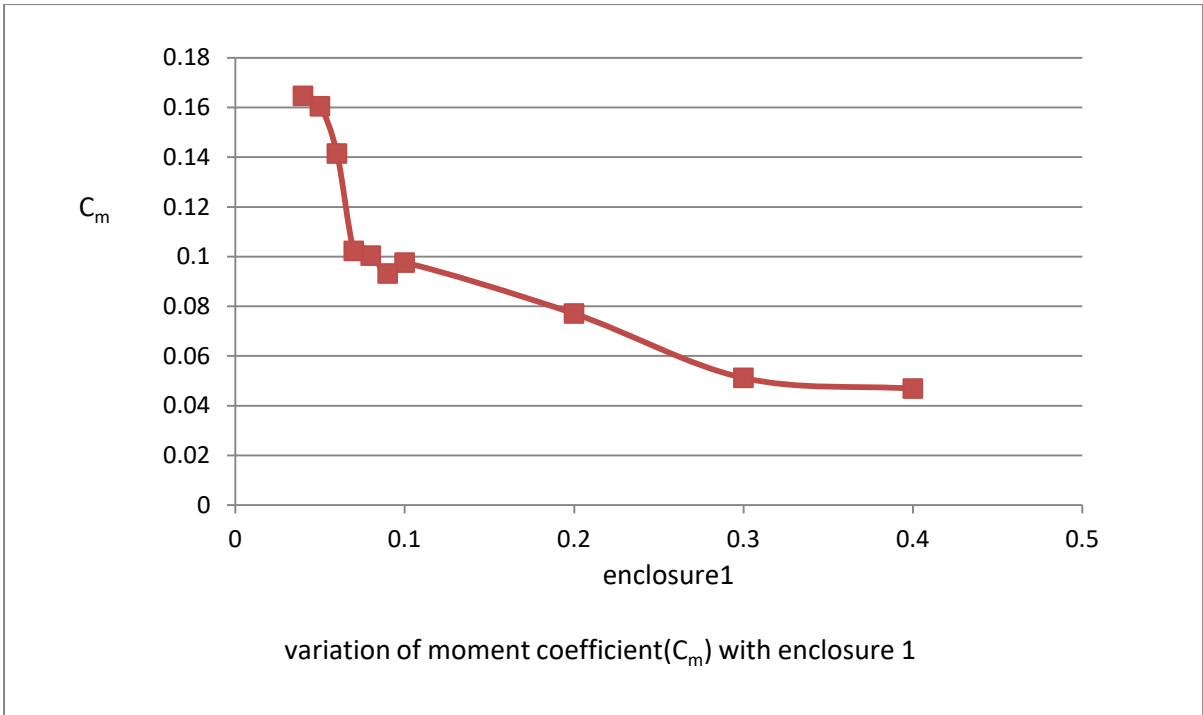


**Figure 4.1** Variation of  $C_m$  with change in enclosure 1

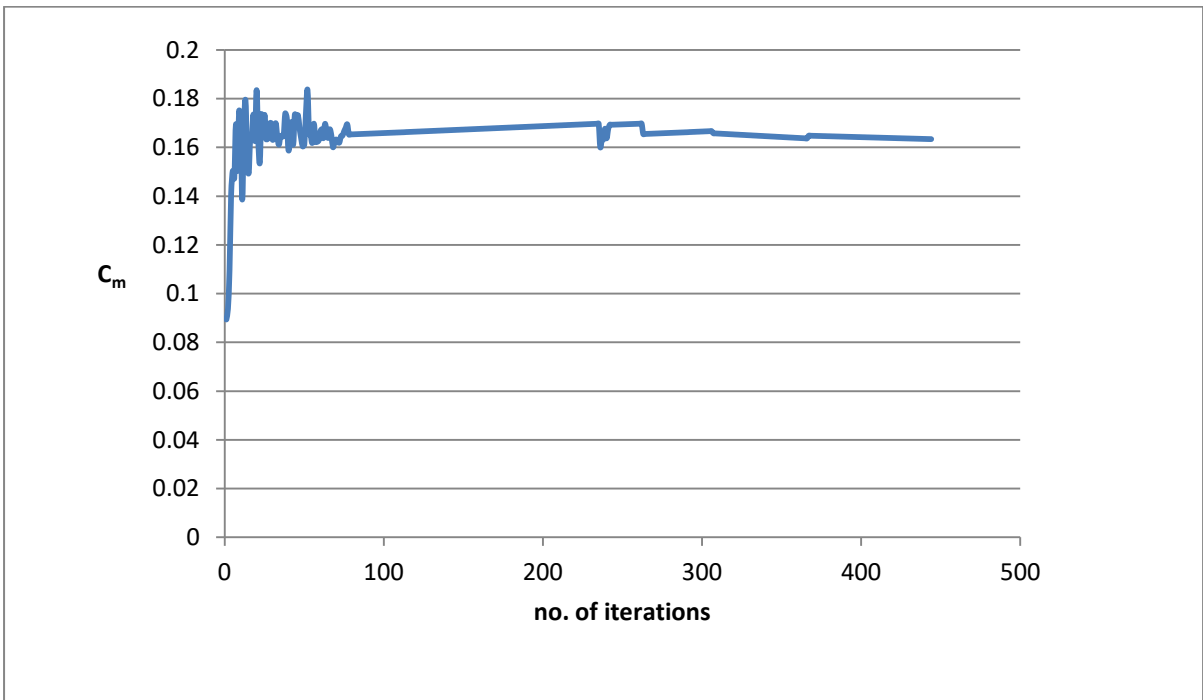


**Figure 4.2**  $C_m$  variation under steady condition

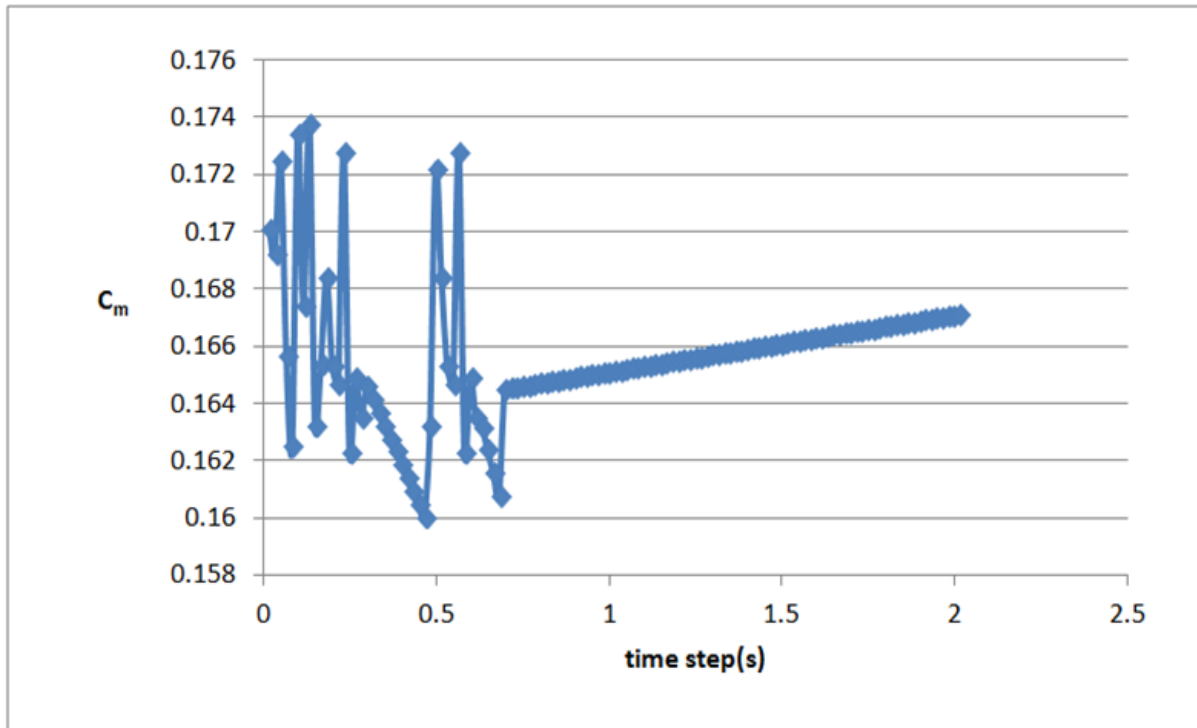


**Figure 4.3**  $C_m$  variation under transient condition

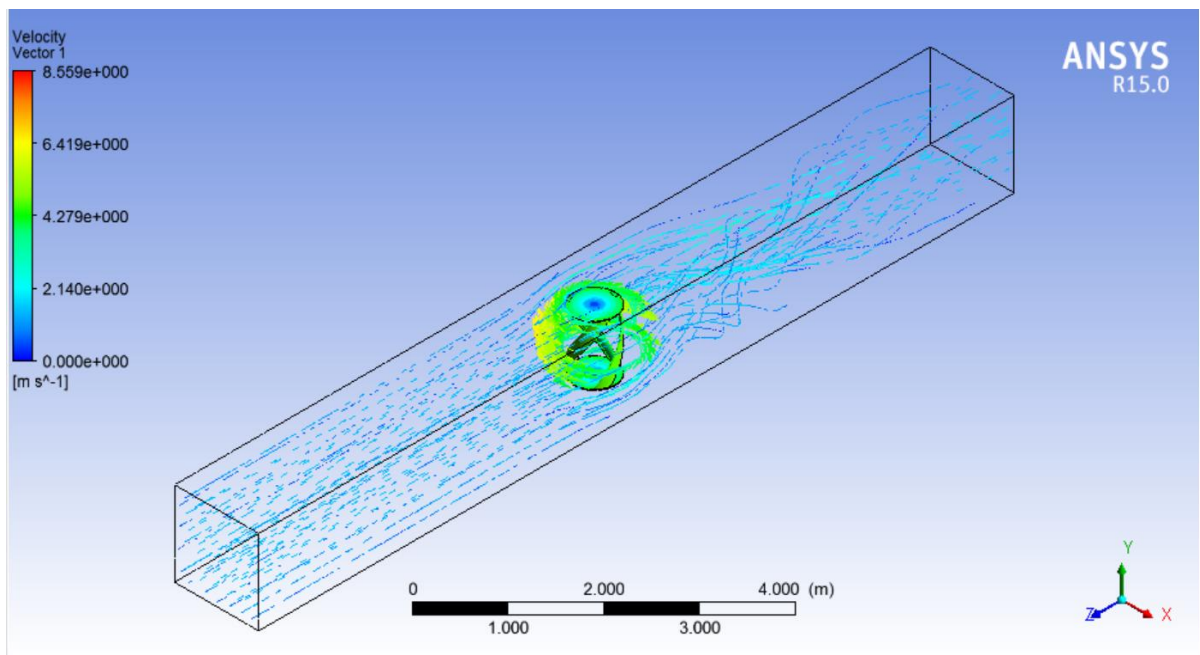


**Figure 4.4** Velocity vectors

From figure 4.4 and 4.5 we can see that velocity is varying from 0 m/s at boundary walls and is reaching to maximum 6.4 m/s around the turbine. Even it is clearly visible from the velocity vector and velocity streamline figure that due to rotation it causes turbulence in the downstream whereas turbine motion does not causes turbulent motion in upstream.

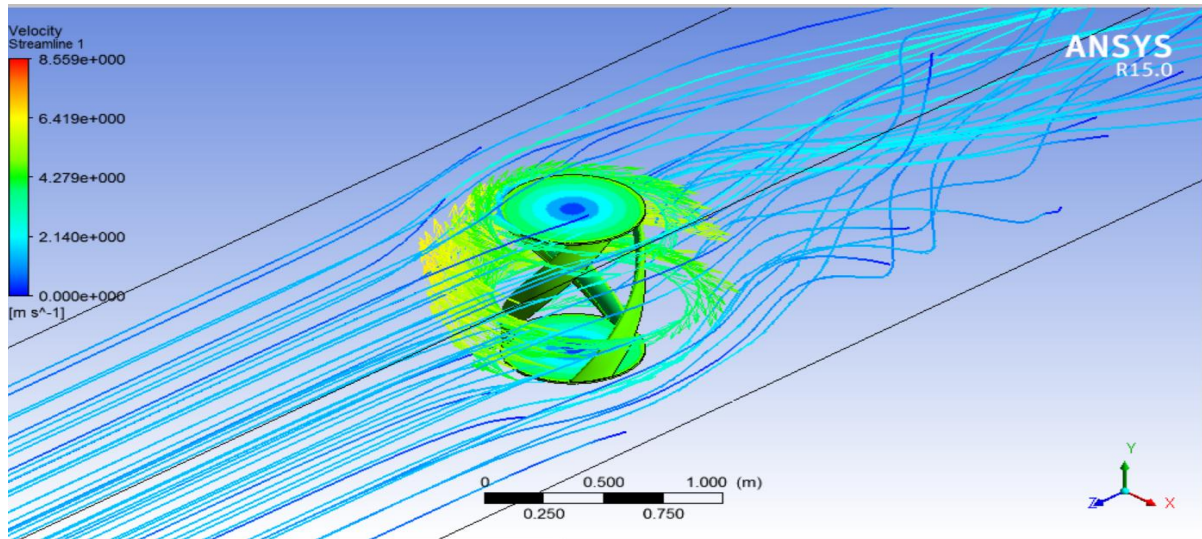


**Figure 4.5** Velocity streamlines

### 4.3 Performance evaluation of helical turbine under varying conditions:

#### 4.3.1. By varying inlet and angular velocity:

On the same Gorlov helical turbine model, boundary conditions were changed i.e. firstly the inlet velocity were changed as 1.5 m/s ,2 m/s and 2.5 m/s and with a particular velocity taken as constant, angular velocity were changed as 100 rpm,110 rpm,120 rpm,130 rpm and 150 rpm.

**Table 4.3** Variation of  $C_m$  on varying inlet & angular velocity

Velocity(m/s) RPM	Velocity(m/s)				
	1.5	1.75	2	2.25	2.5
100	0.1634	0.1622	0.1601	0.166	0.1432
110	0.1731	0.1743	0.1664	0.1500	0.1512
120	0.1842	0.1845	0.1663	0.1729	0.166
130	0.1953	0.1982	0.1910	0.1751	0.1875
140	0.2124	0.2091	0.1837	0.1884	0.1853

<b>150</b>	0.2122	0.2010	0.2046	0.2098	0.1948
------------	--------	--------	--------	--------	--------

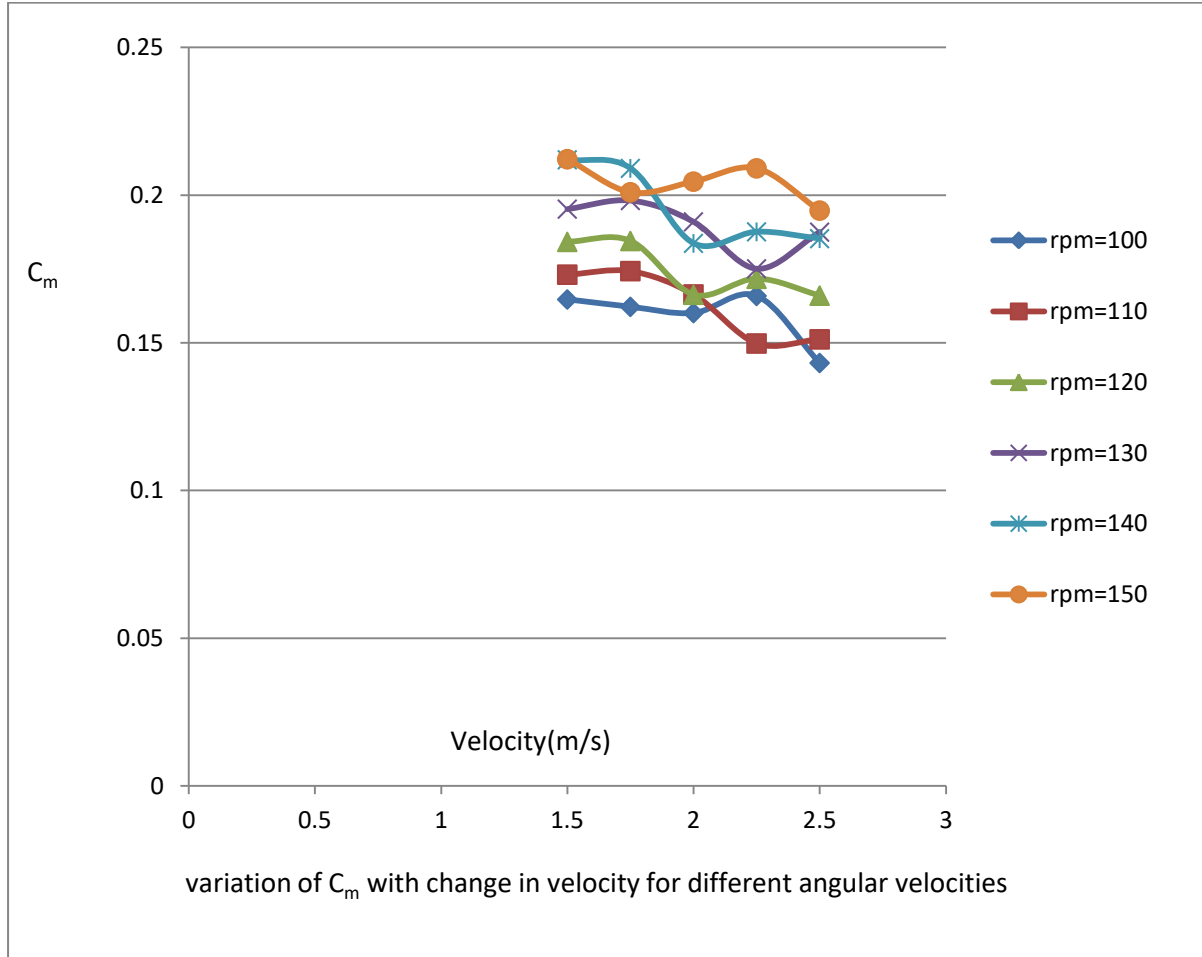


**Figure 4.6**  $C_m$  variation on varying inlet velocity and angular velocity

#### 4.3.2. Performance evaluation by change in volume of turbine:

We have developed ten other models of the helical turbine keeping the Hydrofoil as same i.e. NACA 0020- 7INCH CHORD. To prepare these 10 models we have just slightly changed their aspect ratio so that their volume gets changed. Volume of turbine is calculated as area multiplied by its height which shows the volume of discharge that passes through turbine. Meshing method is kept same as relevance centre being taken as fine. Boundary conditions were also kept same as inlet velocity as 1.5 m/s and angular velocity as 10.47 rpm and K-epsilon model was selected for analysis. Since swept area was unknown therefore it is kept as 0.0081 as default.

**Table 4.4** Ten different helical turbine models detailing

<b>Turbine Model name</b>	<b>Diameter of the helical turbine(metre)</b>	<b>Height of the helical turbine(metre)</b>	<b>Volume of the helical turbine(cubic metre)</b>
V <sub>1</sub>	(20inch)0.508	1.036	0.209873
V <sub>2</sub>	(20.5inch)0.5207	1.011	0.215177
V <sub>3</sub>	(21inch)0.5334	0.9869	0.220419
V <sub>4</sub>	(21.5inch)0.5461	0.964	0.225679
V <sub>5</sub>	(22inch)0.5588	0.9421	0.23093
V <sub>6</sub>	(22.5inch)0.5715	0.9211	0.236161
V <sub>7</sub>	(23inch)0.5842	0.9011	0.241416
V <sub>8</sub>	(23.5inch)0.5969	0.8819	0.246656
V <sub>9</sub>	(24.5inch)0.6263	0.8405	0.258805
V <sub>10</sub>	(25inch)0.635	0.829	0.262405

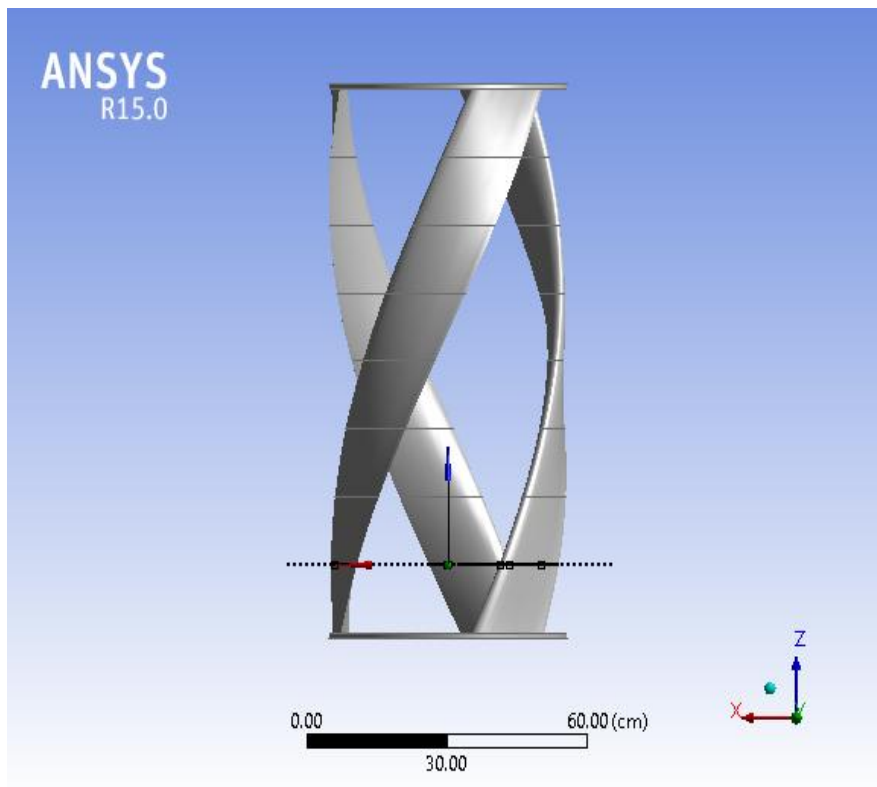


**Figure 4.7** V<sub>1</sub> Model



**Table 4.5** Variation of  $C_m$  by varying turbine dimensions

Diameter of the helical turbine(metres)	Height of the helical turbine(metres)	Volume of the helical turbine(cubic metre)	Moment coefficient ( $C_m$ )
0.5842	0.9011	0.241416	0.1715
0.5588	0.9421	0.23093	0.1805
0.5334	0.9869	0.220419	0.1916
0.508	1.036	0.209873	0.2098
0.5715	0.9211	0.236161	0.1838
0.5461	0.964	0.225679	0.1907
0.5207	1.011	0.215177	0.1937
0.5969	0.8819	0.246656	0.1764
0.6263	0.8405	0.258805	0.1632
0.635	0.829	0.262405	0.1732

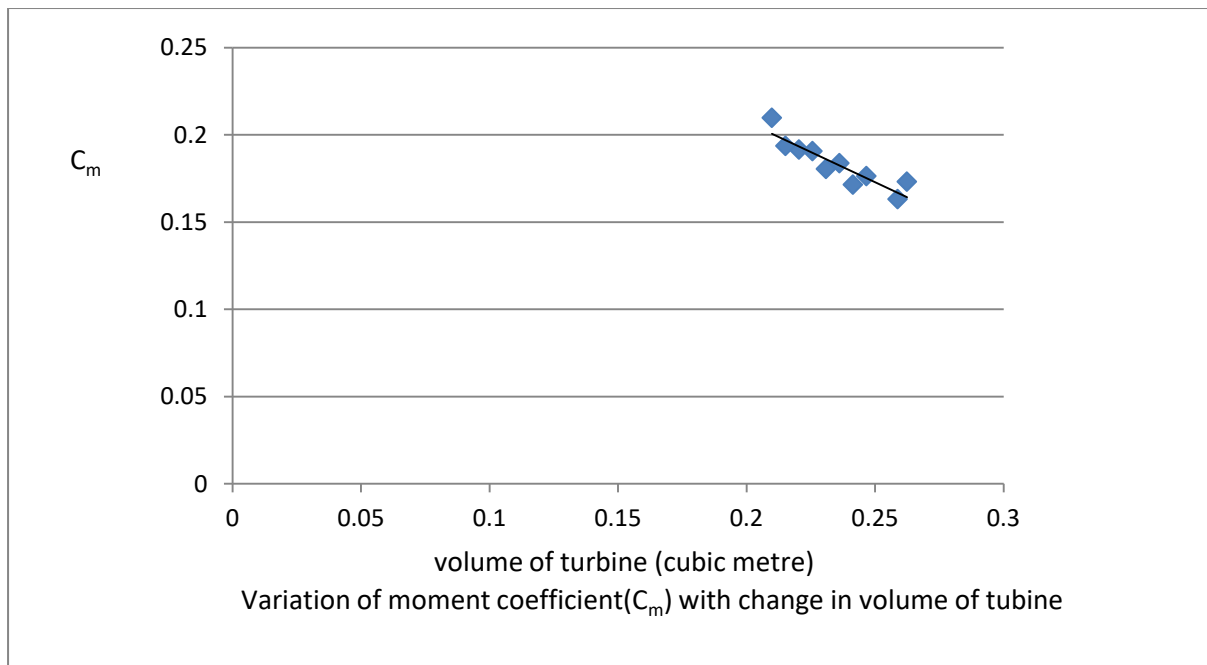


**Figure 4.8**  $C_m$  variation with change in volume of turbine

Results obtained shows that if the volume of discharge passing through turbine increases by

keeping hydrofoil as same, inlet velocity and angular velocity constant then moment coefficient decreases thereby decreasing its efficiency which would result in decrease in power output. A linear regression equation was also developed between moment coefficient as 'y' and volume of turbine as 'x' which is as follows

$$y = -0.6915x + 0.3458 \text{ and } R^2 = 0.8296$$

Where, R is regression coefficient

#### 4.5. Exploration of a possibility of spacing several helical turbines in a line in a river for the purpose of hydropower generations:

Here all the above ten turbine are used and each of them were set at 5m,7.5m,10m,12.5m and 15m and all the boundary conditions were kept same as initial one i.e inlet velocity as 1.5 m/s, angular velocity as 10.47 rad/s, no slip conditions, pressure solver, k-epsilon model etc. Models was designed in ansys design modeller where second model was kept at coordinate (0,0,0) and the first turbine was kept at coordinate (0,0,5) for 5 m spacing, second coordinate was taken simply by shifting the plane along Z- direction as shown in figure 4.9. Turbine at (0,0,5) is turbine 1 on whose  $C_{m-1}$  is found and similarly at origin it is turbine 2 where  $C_{m-2}$  is found. Both the turbine are provided with sphere enclosure 1 as 0.04m by selecting both the turbine individually and then square enclosure 2 as 0.4315 is taken as shown in figure 4.10

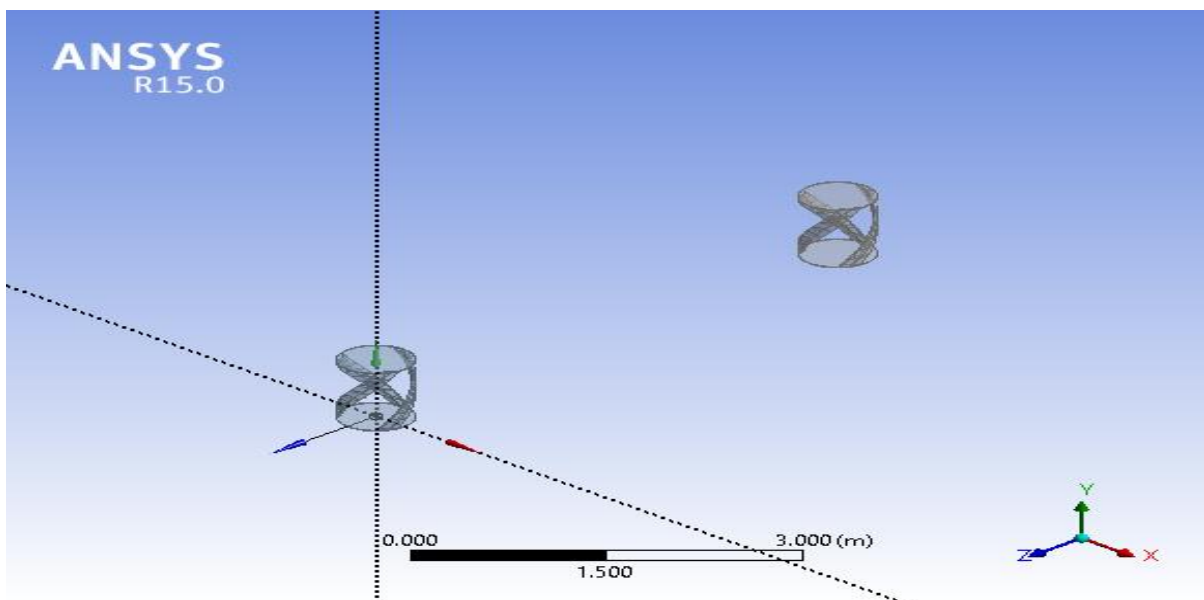
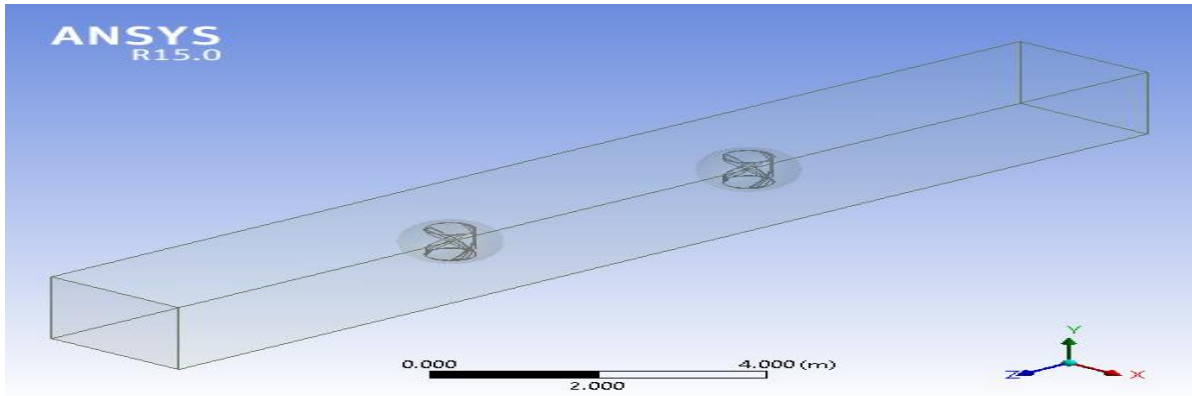
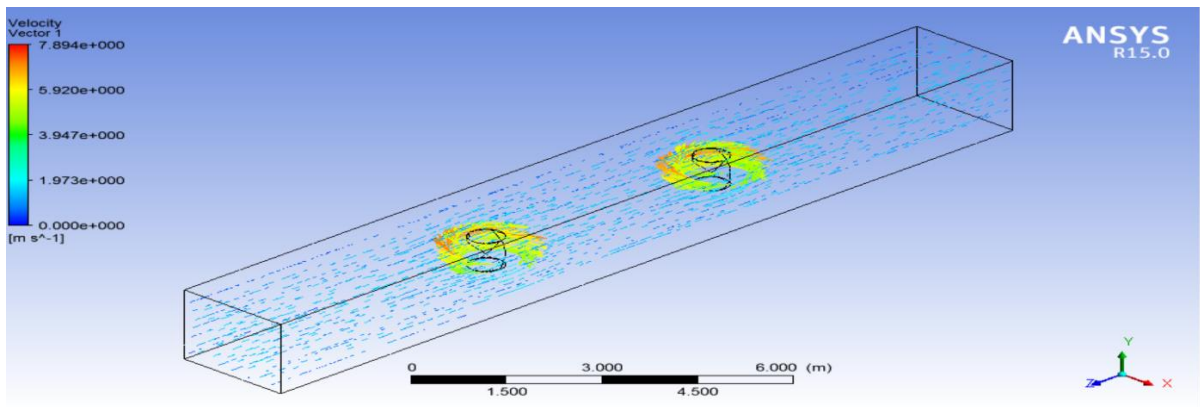


Figure 4.9 Helical position in design modeller



**Figure 4.10** Enclosure in design modeller

Meshing is done again by taking relevance centre as fine method. In results  $C_{m-1}$  is the moment coefficient of the first turbine and  $C_{m-2}$  is the moment coefficient of the second turbine.  $C_{m-1}$  always shows the same value as calculated initially but  $C_{m-2}$  value used to be less when the distance is less and become same as  $C_{m-1}$  when the distance become more than 10m.



**Figure 4.11** Velocity vectors contour for 5 m spacing

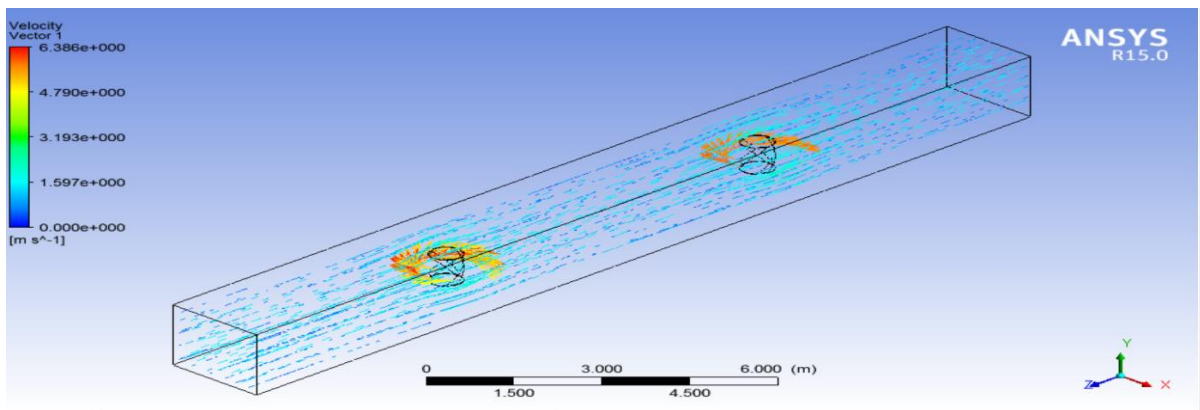


**Figure 4.12** Velocity vectors contour for 7.5 m spacing

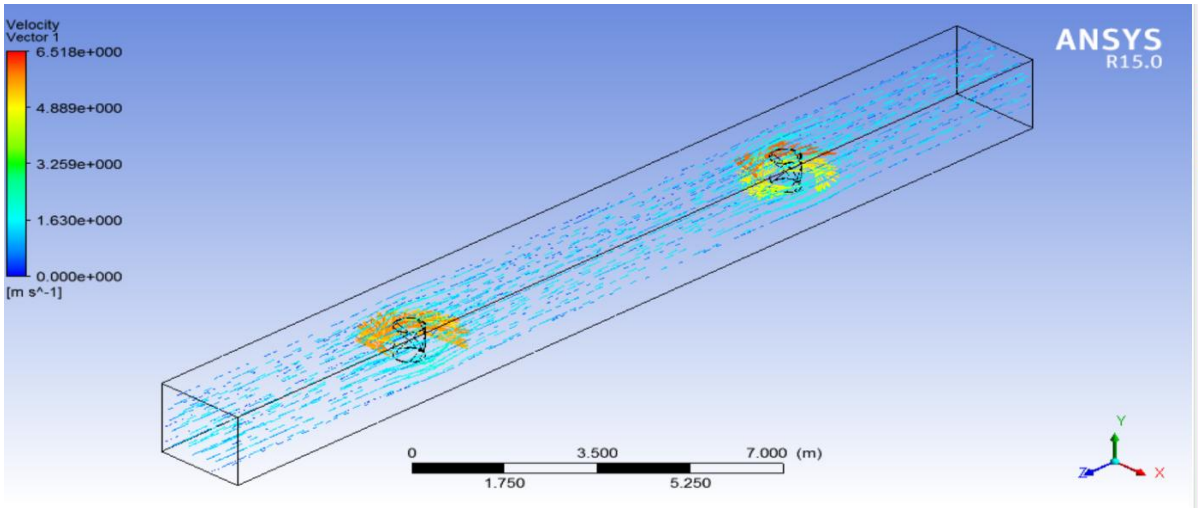


**Figure 4.13** Velocity vectors contour for 10 m spacing

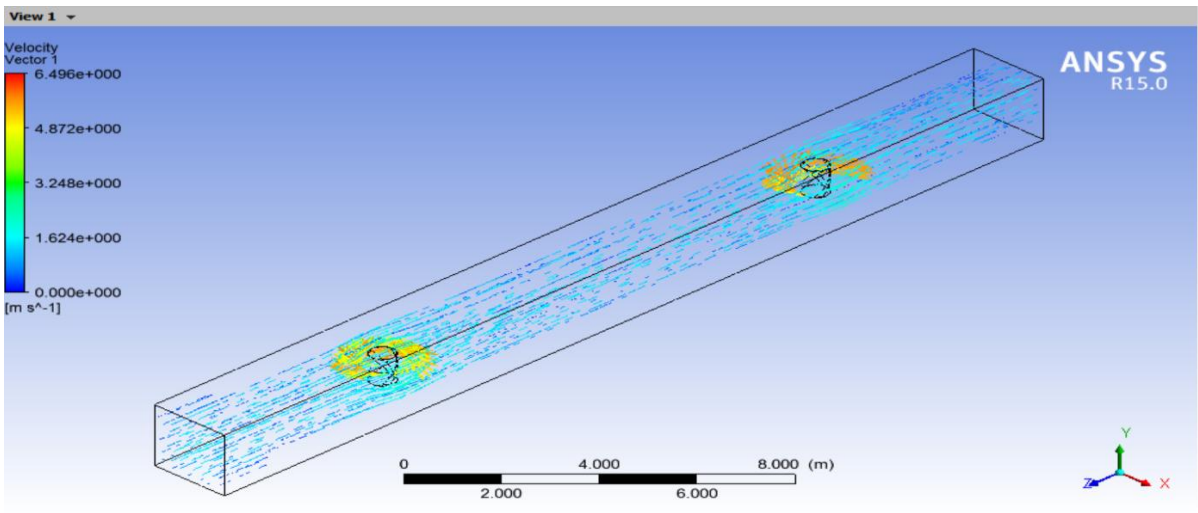


**Figure 4.14** Velocity vectors contour for 12.5 m spacing

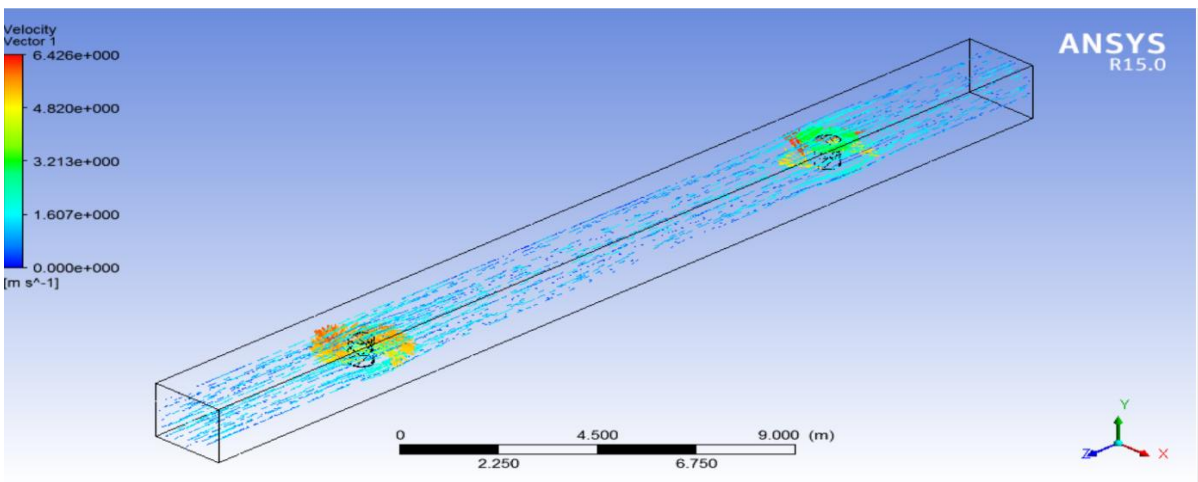


**Figure 4.15** Velocity vectors contour for 15 m spacing

**Table 4.6** Variation of  $C_m-1$  &  $C_m-2$  with change in spacing for model  $V_1$

<b>Volume of turbine (cubic metre)</b>	<b>Spacing (metres)</b>	<b><math>C_m-1</math></b>	<b><math>C_m-2</math></b>	<b>value of <math>C_m</math> taken for interpolation</b>	<b>desired value of spacing (metres)</b>
0.209873	5	0.2161	0.1133	0.21	15
	7.5	0.1978	0.1602		
	10	0.2096	0.1831		
	12.5	0.21	0.1987		
	15	0.2101	0.2101		

**Table 4.7** Variation of  $C_m-1$  &  $C_m-2$  with change in spacing for model  $V_2$

<b>Volume of turbine (cubic metre)</b>	<b>Spacing (metres)</b>	<b><math>C_m-1</math></b>	<b><math>C_m-2</math></b>	<b>value of <math>C_m</math> taken for interpolation</b>	<b>desired value of spacing (metres)</b>
0.215177	5	0.1906	0.0824	0.19	14.67
	7.5	0.199	0.0963		
	10	0.1905	0.1326		
	12.5	0.1902	0.1827		
	15	0.1905	0.1911		

**Table 4.8** Variation of  $C_m-1$  &  $C_m-2$  with change in spacing for model  $V_3$ 

<b>Volume of turbine (cubic metre)</b>	<b>Spacing (metres)</b>	<b><math>C_m-1</math></b>	<b><math>C_m-2</math></b>	<b>value of <math>C_m</math> taken for interpolation</b>	<b>desired value of spacing (metres)</b>
0.220419	5	0.1976	0.1197	0.19	12.48
	7.5	0.1925	0.1451		
	10	0.1946	0.1754		
	12.5	0.1992	0.1901		
	15	0.1945	0.1914		

**Table 4.9** Variation of  $C_m-1$  &  $C_m-2$  with change in spacing for model  $V_4$ 

<b>Volume of turbine (cubic metre)</b>	<b>Spacing (metres)</b>	<b><math>C_m-1</math></b>	<b><math>C_m-2</math></b>	<b>value of <math>C_m</math> taken for interpolation</b>	<b>desired value of spacing (metres)</b>
0.225679	5	0.1906	0.0824	0.19	15
	7.5	0.199	0.0963		
	10	0.1905	0.1326		
	12.5	0.1915	0.1827		
	15	0.1905	0.19		

**Table 4.10** Variation of  $C_{m-1}$  &  $C_{m-2}$  with change in spacing for model  $V_5$ 

<b>Volume of turbine (cubic metre)</b>	<b>Spacing (metres)</b>	<b><math>C_{m-1}</math></b>	<b><math>C_{m-2}</math></b>	<b>value of <math>C_m</math> taken for interpolation</b>	<b>desired value of spacing (metres)</b>
0.23093	5	0.1841	0.0913	0.18	12.43
	7.5	0.184	0.1379		
	10	0.1812	0.1639		
	12.5	0.181	0.1804		
	15	0.1811	0.1831		

**Table 4.11** Variation of  $C_{m-1}$  &  $C_{m-2}$  with change in spacing for model  $V_6$ 

<b>Volume of turbine (cubic metre)</b>	<b>Spacing (metres)</b>	<b><math>C_{m-1}</math></b>	<b><math>C_{m-2}</math></b>	<b>value of <math>C_m</math> taken for interpolation</b>	<b>desired value of spacing (metres)</b>
0.236161	5	0.1819	0.1017	0.18	12.55
	7.5	0.1839	0.1214		
	10	0.1839	0.1559		
	12.5	0.1829	0.1799		
	15	0.1819	0.1842		

**Table 4.12** Variation of  $C_{m-1}$  &  $C_{m-2}$  with change in spacing for model  $V_7$

<b>Volume of turbine (cubic metre)</b>	<b>Spacing (metres)</b>	<b><math>C_{m-1}</math></b>	<b><math>C_{m-2}</math></b>	<b>value of <math>C_m</math> taken for interpolation</b>	<b>desired value of spacing (metres)</b>
0.241416	5	0.1795	0.1112	0.17	12.26
	7.5	0.1718	0.1401		
	10	0.1716	0.1631		
	12.5	0.1716	0.1707		
	15	0.1717	0.1715		

**Table 4.13** Variation of  $C_{m-1}$  &  $C_{m-2}$  with change in spacing for model  $V_8$

<b>Volume of turbine (cubic metre)</b>	<b>Spacing (metres)</b>	<b><math>C_{m-1}</math></b>	<b><math>C_{m-2}</math></b>	<b>value of <math>C_m</math> taken for interpolation</b>	<b>desired value of spacing (metres)</b>
0.246056	5	0.179	0.1248	0.17	12.47
	7.5	0.176	0.1272		
	10	0.172	0.1612		
	12.5	0.1712	0.1701		
	15	0.1727	0.1732		



**Table 4.14** Variation of  $C_{m-1}$  &  $C_{m-2}$  with change in spacing for model  $V_9$ 

<b>Volume of turbine (cubic metre)</b>	<b>Spacing (metres)</b>	<b><math>C_{m-1}</math></b>	<b><math>C_{m-2}</math></b>	<b>value of <math>C_m</math> taken for interpolation</b>	<b>desired value of spacing (metres)</b>
0.258805	5	0.1632	0.1101	0.16	12.604
	7.5	0.1632	0.1357		
	10	0.1621	0.1583		
	12.5	0.1675	0.1599		
	15	0.164	0.1623		

**Table 4.15** Variation of  $C_{m-1}$  &  $C_{m-2}$  with change in spacing for model  $V_{10}$ 

<b>Volume of turbine (cubic metre)</b>	<b>Spacing (metres)</b>	<b><math>C_{m-1}</math></b>	<b><math>C_{m-2}</math></b>	<b>value of <math>C_m</math> taken for interpolation</b>	<b>desired value of spacing (metres)</b>
0.262405	5	0.1737	0.1069	0.17	12.37
	7.5	0.1787	1272		
	10	0.174	0.1522		
	12.5	0.1739	0.1709		
	15	0.1734	0.1738		

A linear regression equation has been derived between volume of turbine in metres as “y” and the desired spacing in metres as “x” as following.

$$y = -45.84x + 23.942, R^2 = 0.4694$$

Where, R is regression constant.

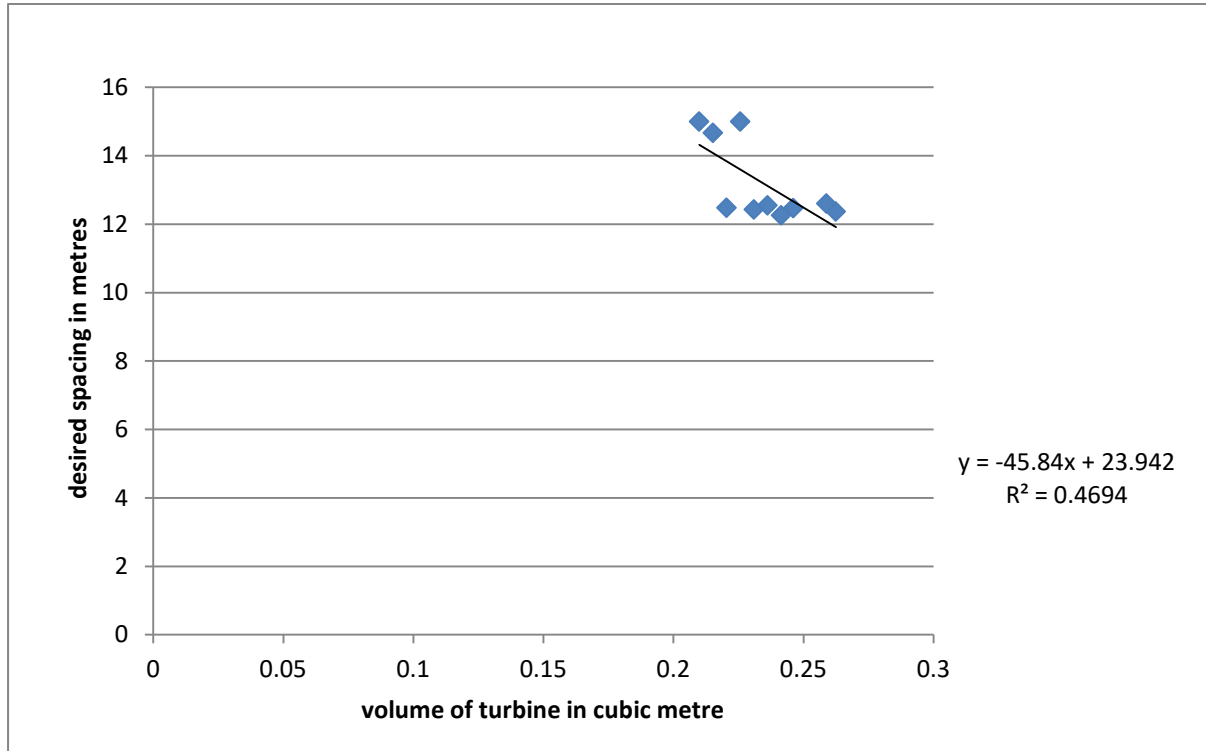


**Figure 4.16** Graph on desired spacing with the variation in volume of turbine

#### **4.6. Effects of helical turbine operation in variation of flow velocity in channel upstream and downstream side.**

As it has been observed in spacing case that  $C_m-2$  value was coming out to be same as  $C_m-1$  above 12.5 m and was decreasing below it therefore velocity variation in the channel was observed in the upstream and downstream channel when helical turbine operates with angular velocity as 10.47 rad/sec and inlet velocity as 1.5 m/sec. Therefore a model is developed by keeping Gorlov helical turbine and making upstream and downstream channel as 20 m each. Meshing and boundary conditions were kept same as initial i.e inlet velocity as 1.5 m/s, at outlet section weighted factor 1, walls being taken as hydro dynamically smooth, angular velocity of turbine is taken as 100 rpm, pressure solver is used with K-epsilon turbulence model.

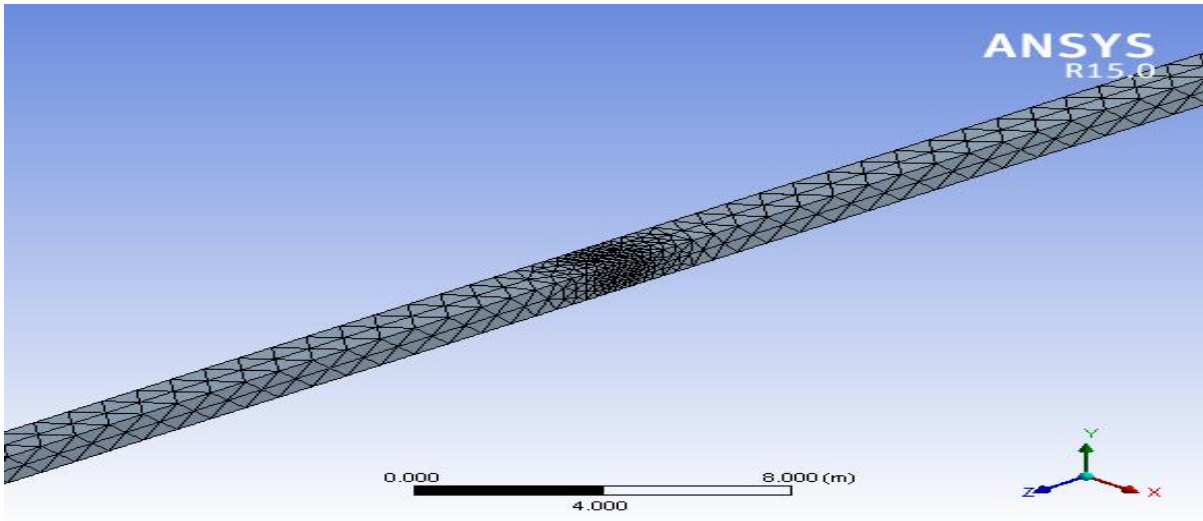


**Figure 4.17** Mesh diagram for 40 m channel

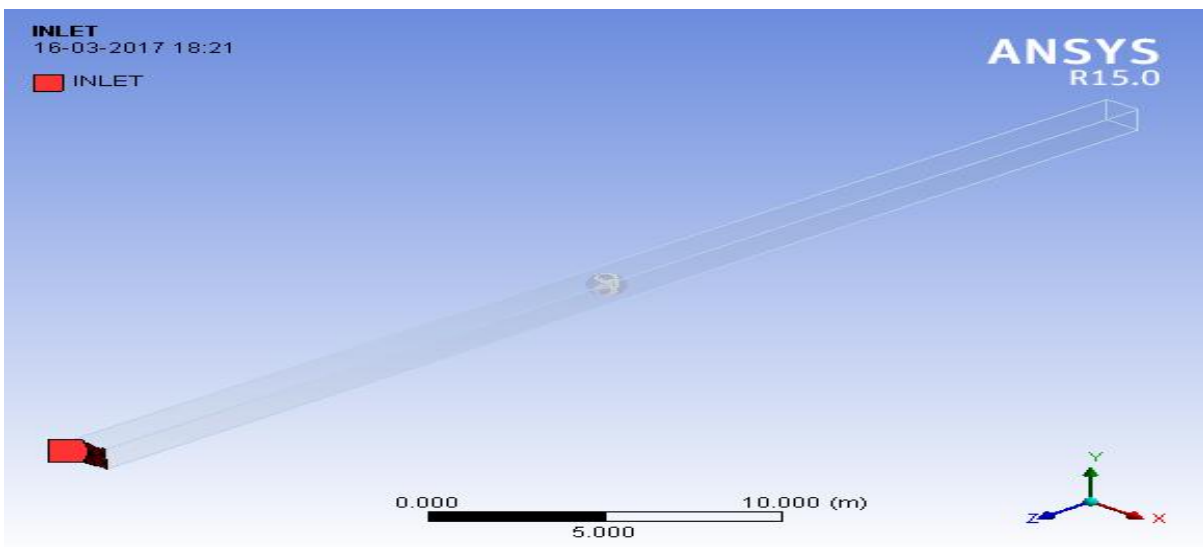


**Figure 4.18** Inlet for 40 m channel model

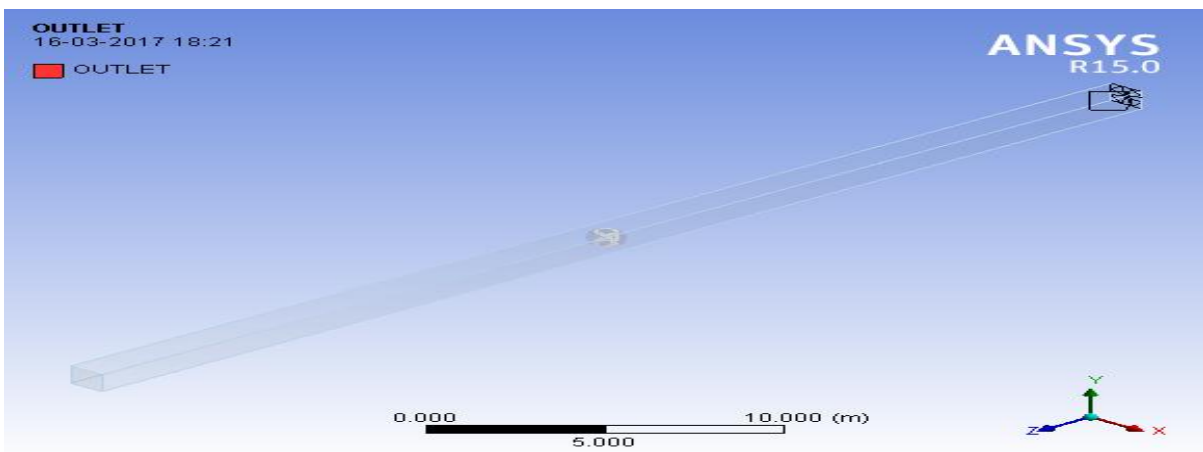


**Figure 4.19** Outlet for 40 m channel model

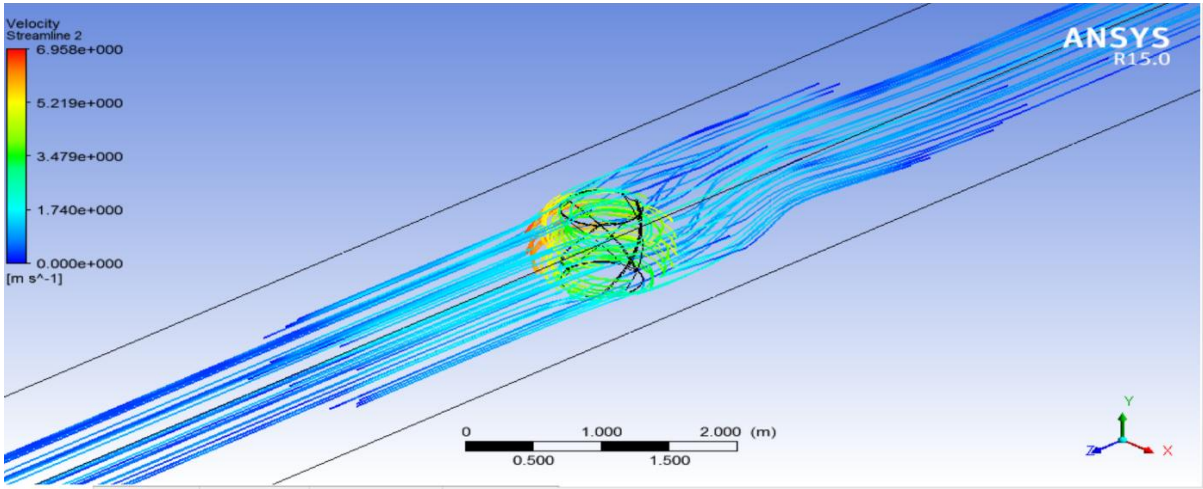


**Figure 4.20** Velocity streamlines for 40 m channel

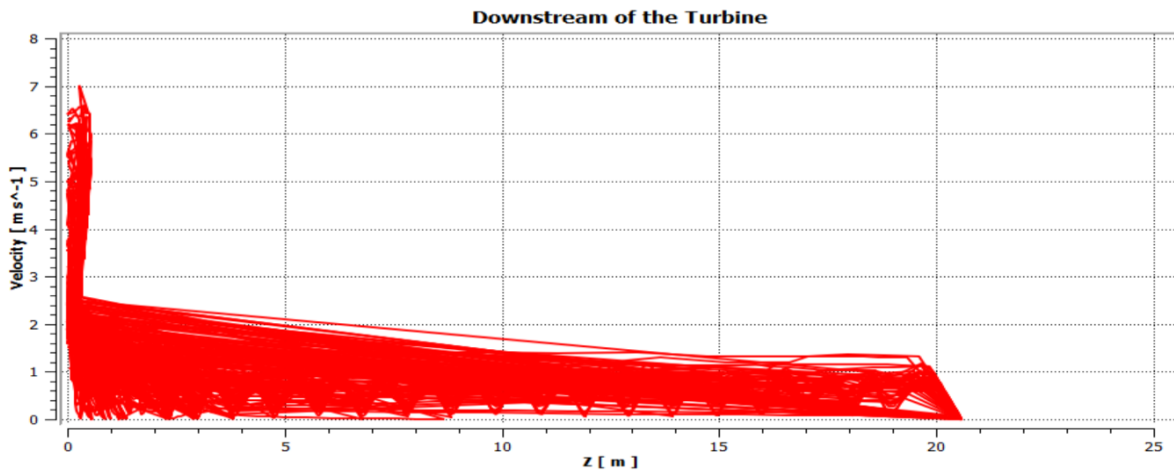


**Figure 4.21** Velocity variation chart for channel in downstream of turbine

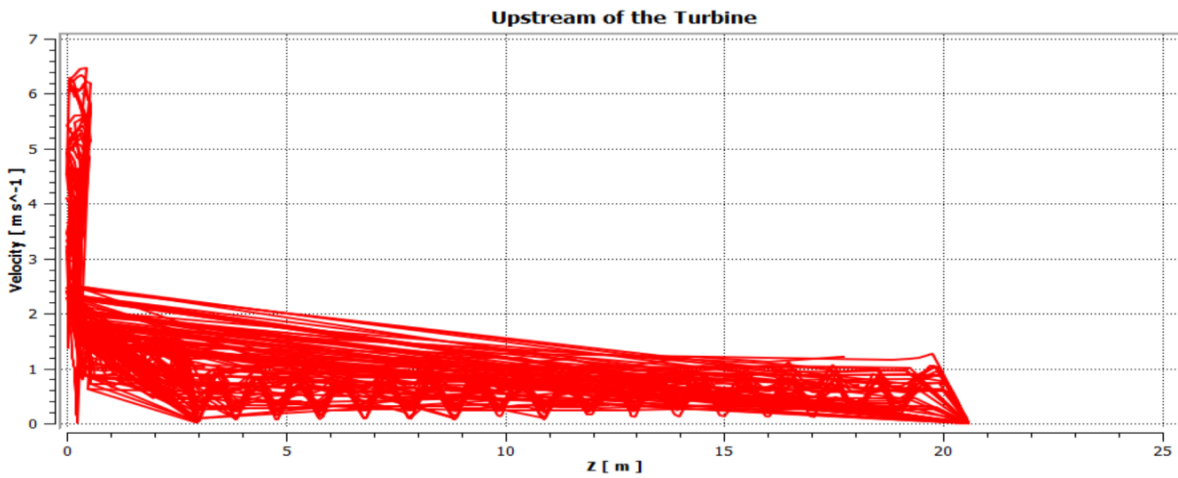


**Figure 4.22** Velocity chart for channel in upstream of turbine

Here Figure 4.20 shows that velocity streamlines are parallel upstream to the turbine whereas it is showing turbulent effect in downstream portion only and that too up to 1.5 m only. But when velocity graph was taken out for downstream and upstream channel in the Z direction which is the flow direction as figure 4.21 and 4.22 respectively, which actually shows different velocity line that are there in x-direction. Which means that even there exists a little turbulence in velocity of fluid elements up to 10 m which is maximum in the 1m upstream and downstream side. It also shows that at downstream side velocity becomes same as 1.5 m/s at approximately around 15m whereas in upstream portion it becomes same at approximately around 12.5m.

## Chapter 5 CONCLUSIONS

- 1) CFD model of helical turbine was made using ansys fluent.
- 2) Model was validated with Gorlov Model results.
- 3) CFD studies were conducted on turbine by varying inlet velocity as 1.5 m/s to 2.5 m/s with a step size of 0.25 m/s and angular velocity from 100 to 150 rpm with a step size of 10 rpm and it was found that with increase in inlet velocity keeping angular velocity constant, moment coefficient  $C_m$  was decreasing which means decrease in efficiency, whereas with increase in RPM keeping inlet velocity constant, moment coefficient  $C_m$  increases which means increase in efficiency
- 4) CFD analysis was carried out by placing two turbines in a line and the spacing between the turbine was varied from 5-15m with a step of 2.5 m and the volume of the two turbine in a line from 0.20 cubic metre to 0.26 cubic metres and it was found the that spacing between the turbines was coming to be 11 to 13 m and a linear regression model has been developed between volume of turbine in cubic metres  $m$  as 'x' and desired spacing in metres as 'y':

$$y = -45.84x + 23.942$$

$$R^2 = 0.4694$$

- 5) CFD analysis to determine the effect in the variation of flow is carried out when a helical turbine is in operation condition and it was found that in upstream region up to 0.5 m, velocity goes to 6m/s and its stabilises at 12.5 m upstream of it, whereas in downstream channel up to 0.5 m, velocity goes to 7 m/s up to 0.5m and it stabilises at approx 15 m downstream, Whereas turbulence effects is being shown in both upstream and downstream portions.

## REFERENCES

- 1) Adam I. Niblick “*experimental and analytical study of helical cross-flow turbines for a tidal micro power generation system*”, university of Washington, 2012.
- 2) Andrea Alaimo, Antonio Esposito, Antonio Messineo, Calogero Orlando and Davide Tumino “*3d cfd analysis of a vertical axis wind turbine*” research gate, 2015.
- 3) A. Reza Hassanzadeh, Omar Yaakob, Yasser M. Ahmed and M. Arif Ismail, “*comparison of conventional and helical savonius marine current turbine using computational fluid dynamics*” world applied sciences journal, 2013.
- 4) Bachu Deb, Rajat Gupta and R.D. Misra “*performance analysis of a helical savonius rotor without shaft at 45° twist angle using cfd*” journal of urban and environmental engineering, vol.7,2013.
- 5) David Hartwanger and D Andrej Horvat “*3D modelling of wind turbine using cfd*” NAFEMS UK Conference 2008 "Engineering Simulation: Effective Use and Best Practice",2008
- 6) Dibakara reddy, Surender Singh, Tejeshwar Reddy “*CFD analysis on a savonius rotor wind turbine made using mild steel material*” international journal of mechanical and production engineering, volume- 4,2016.
- 7) Dr. Alexander Gorlov “*Development of the helical reaction hydraulic turbine, US Department of energy*” 1998.
- 8) Himanshu joshi, Arpit Dwivedi, Anish Anand, Pravin p. patil “*design and analysis of a cross flow hydrokinetic turbine using computational fluid dynamics*” journal of basic and applied engineering research, vol.1,2014.
- 9) Md. Intiaj Hassan, Tariq Iqbal, Nahidul khan, Michael Hinchey, Vlastimil Masek “*cfd analysis of a twisted savonius turbine*” memorial university of Newfoundland, Canada.
- 10) Mr.Laxmikant N.Dhoble, Dr.A.K.Mahalle “*cfd analysis of savonius vertical axis wind turbine*” a review, international research journal of engineering and technology (irjet), vol.3, 2016.
- 11) Md. Saddam Hussien, D R. K. rambabu, M. Ramji , E. Srinivas “*Design and Analysis of vertical axis wind turbine rotors*” international journal on recent technologies in mechanical and electrical engineering, vol.2,2015.
- 12) Nor Afzanizam Bin Hj. Samiran “*simulation study on the performance of vertical axis wind turbine*” university tun Hussein onn Malaysia, 2013.

- 13) Travis E. Salyers “*experimental and numerical investigation of aerodynamic performance for vertical-axis wind turbine models with various blade designs*” Georgia southern university, 2016.
- 14) Tuyen Quang Le, Kwang-Soo Lee, Jin-Soon Park and Jin Hwan Ko “*flow driven rotor simulation of vertical axis tidal turbines: a comparison of helical and straight blades*” int.j.nav.archit.ocean eng., vol.6, 2014.